

## $\beta$ -delayed neutron emissions from $N > 50$ gallium isotopes

R. Yokoyama,<sup>1,2,\*</sup> R. Grzywacz,<sup>1,3</sup> B. C. Rasco,<sup>3,1</sup> N. Brewer,<sup>3,1</sup> K. P. Rykaczewski,<sup>3</sup> I. Dillmann,<sup>4</sup> J. L. Tain,<sup>5</sup> S. Nishimura,<sup>6</sup> D. S. Ahn,<sup>6</sup> A. Algora,<sup>5,7</sup> J. M. Allmond,<sup>3</sup> J. Agramunt,<sup>5</sup> H. Baba,<sup>6</sup> S. Bae,<sup>8</sup> C. G. Bruno,<sup>9</sup> R. Caballero-Folch,<sup>4</sup> F. Calvino,<sup>10</sup> P. J. Coleman-Smith,<sup>11</sup> G. Cortes,<sup>10</sup> T. Davinson,<sup>9</sup> C. Domingo-Pardo,<sup>5</sup> A. Estrade,<sup>12</sup> N. Fukuda,<sup>6</sup> S. Go,<sup>6</sup> C. J. Griffin,<sup>9</sup> J. Ha,<sup>13,6</sup> O. Hall,<sup>9</sup> L. J. Harkness-Brennan,<sup>14</sup> J. Heideman,<sup>1</sup> T. Isobe,<sup>6</sup> D. Kahl,<sup>9</sup> M. Karny,<sup>15</sup> T. Kawano,<sup>16</sup> L. H. Khiem,<sup>17</sup> T. T. King,<sup>1</sup> G. G. Kiss,<sup>6,7</sup> A. Korgul,<sup>15</sup> S. Kubono,<sup>6</sup> M. Labiche,<sup>11</sup> I. Lazarus,<sup>11</sup> J. Liang,<sup>18</sup> J. Liu,<sup>19,6</sup> G. Lorusso,<sup>20,21,6</sup> M. Madurga,<sup>1</sup> K. Matsui,<sup>6,22</sup> K. Miernik,<sup>15</sup> F. Montes,<sup>23</sup> A. I. Morales,<sup>5</sup> P. Morrall,<sup>11</sup> N. Nepal,<sup>12</sup> R. D. Page,<sup>14</sup> V. H. Phong,<sup>6,24</sup> M. Piersa-Silkowska,<sup>15</sup> M. Prydderch,<sup>25</sup> V. F. E. Pucknell,<sup>11</sup> M. M. Rajabali,<sup>26</sup> B. Rubio,<sup>5</sup> Y. Saito,<sup>4</sup> H. Sakurai,<sup>6</sup> Y. Shimizu,<sup>6</sup> J. Simpson,<sup>11</sup> M. Singh,<sup>1</sup> D. W. Stracener,<sup>3</sup> T. Sumikama,<sup>6</sup> H. Suzuki,<sup>6</sup> H. Takeda,<sup>6</sup> A. Tarifeño-Saldivia,<sup>10</sup> S. L. Thomas,<sup>25</sup> A. Tolosa-Delgado,<sup>5</sup> M. Wolińska-Cichocka,<sup>27</sup> P. J. Woods,<sup>9</sup> and X. X. Xu<sup>19</sup>

<sup>1</sup>*Department of Physics and Astronomy, University of Tennessee, Knoxville, TN 37996, USA*

<sup>2</sup>*Center for Nuclear Study, the University of Tokyo, 2-1 Hirosawa, Wako, Saitama 351-0198, Japan*

<sup>3</sup>*Physics Division, Oak Ridge National Laboratory, Oak Ridge, TN 37830, USA*

<sup>4</sup>*TRIUMF, Vancouver, British Columbia V6T 2A3, Canada*

<sup>5</sup>*Instituto de Fisica Corpuscular (CSIC-Universitat de Valencia), E-46071 Valencia, Spain*

<sup>6</sup>*RIKEN, Nishina Center, 2-1 Hirosawa, Wako, Saitama 351-0198, Japan*

<sup>7</sup>*MTA Atomki, Bem ter 18/c, Debrecen H4032, Hungary*

<sup>8</sup>*Center for Exotic Nuclear Studies, Institute for Basic Science, 55 EXPO-ro, Yuseong-gu, Daejeon, 34126, Republic of Korea*

<sup>9</sup>*School of Physics and Astronomy, University of Edinburgh, EH9 3FD Edinburgh, UK*

<sup>10</sup>*Universitat Politècnica de Catalunya (UPC), E-08028 Barcelona, Spain*

<sup>11</sup>*STFC Daresbury Laboratory, Daresbury, Warrington WA4 4AD, UK*

<sup>12</sup>*Department of Physics and Science of Advanced Materials Program, Central Michigan University, Mount Pleasant, MI 48859, USA*

<sup>13</sup>*Department of Physics and Astronomy, Seoul National University, 1 Gwanak-ro, Gwanak-gu, Seoul 08826, Republic of Korea*

<sup>14</sup>*Department of Physics, University of Liverpool, Liverpool L69 7ZE, UK*

<sup>15</sup>*Faculty of Physics, University of Warsaw, PL-02-093 Warsaw, Poland*

<sup>16</sup>*Los Alamos National Laboratory, Los Alamos, NM 87545, USA*

<sup>17</sup>*Institute of Physics, Vietnam Academy of Science and Technology, 10 Dao Tan, Ba Dinh, Ha Noi, Viet Nam*

<sup>18</sup>*Department of Physics and Astronomy, McMaster University, Hamilton, Ontario L8S 4M1, Canada*

<sup>19</sup>*Department of Physics, the University of Hong Kong, Pokfulam Road, Hong Kong*

<sup>20</sup>*National Physical Laboratory (NPL), Teddington, Middlesex TW11 0LW, UK*

<sup>21</sup>*Department of Physics, University of Surrey, Guildford, GU2 7XH, UK*

<sup>22</sup>*Department of Physics, the University of Tokyo, 7-3-1 Hongo, Bunkyo-ku, Tokyo 113-0033, Japan*

<sup>23</sup>*National Superconducting Cyclotron Laboratory,*

*Michigan State University, East Lansing, MI 48824, USA*

<sup>24</sup>*University of Science, Vietnam National University, Hanoi 120062, Vietnam*

<sup>25</sup>*STFC Rutherford Appleton Laboratory, Harwell Campus, Didcot OX11 0QX, UK*

<sup>26</sup>*Department of Physics, Tennessee Technological University, Cookeville, TN 38505, USA*

<sup>27</sup>*Heavy Ion Laboratory, University of Warsaw, Warsaw PL-02-093, Poland*

(Dated: November 13, 2023)

$\beta$ -delayed  $\gamma$ -neutron spectroscopy has been performed on the decay of  $A = 84$  to  $87$  gallium isotopes at the RI-beam Factory at the RIKEN Nishina Center using a high-efficiency array of  $^3\text{He}$  neutron counters (BRIKEN).  $\beta$ -2n- $\gamma$  events were measured in the decays of all of the four isotopes for the first time, which is direct evidence for populating the excited states of two-neutron daughter nuclei. Detailed decay schemes with the  $\gamma$  branching ratios were obtained for these isotopes and the neutron emission probabilities ( $P_{xn}$ ) were updated from the previous study. Hauser-Feshbach statistical model calculations were performed to understand the experimental branching ratios. We found that the  $P_{1n}$  and  $P_{2n}$  values are sensitive to the nuclear level densities of In daughter nuclei and showed that the statistical model reproduced the  $P_{2n}/P_{1n}$  ratio better when experimental levels + shell-model level densities fit by the Gilbert-Cameron formula were used as the level-density input. We also showed the neutron and  $\gamma$  branching ratios are sensitive to the ground-state spin of the parent nucleus. Our statistical model analysis suggested  $J \leq 3$  for the unknown ground-state spin of the odd-odd nucleus,  $^{86}\text{Ga}$ , from the  $I_\gamma(4^+ \rightarrow 2^+)/I_\gamma(2^+ \rightarrow 0^+)$  ratio of  $^{84}\text{Ga}$  and the  $P_{2n}/P_{1n}$  ratio. These results show the necessity of detailed understanding of the decay scheme, including data from neutron spectroscopy, in addition to  $\gamma$  measurements of the multi-neutron emitters.

## I. INTRODUCTION

$\beta$ -delayed neutron emission is a decay mode found in very neutron-rich nuclei where the energy window of the  $\beta$ -decay ( $Q_\beta$ ) is high enough to populate excited states of the daughter nucleus above neutron separation energy ( $S_n$ ). This process was first observed in 1939 [1], and there have been 300 one-neutron emitters found [2, 3]. Moving further away from the line of stability to more neutron-rich nuclei, the  $Q_\beta$  increases rapidly and neutron separation energies continue to decrease, which makes delayed multi-neutron emission energetically available.

The number of neutrons emitted in decays of neutron-rich nuclei is an important input for astrophysical  $r$ -process abundance calculations. It affects the final isobaric abundance pattern by providing neutrons for the late-time captures process and changing the decay path back to stability [4]. Until recently, the neutron emission probabilities for the  $r$ -process abundance calculations relied on predictions based on the simplified assumption that only  $x$ -neutron emission will occur when  $\beta$ -decay fed a state above  $S_{xn}$ , and the effect of less-than- $x$ -neutron channels are negligible. We call this simplified approach the ‘‘cutoff’’ model. In this model, the neutron emission probabilities are proportional to the integrated population of states in the available energy window,  $Q_\beta - S_{(x+1)n} < E_\beta < Q_\beta - S_n$ , and are directly related to the  $\beta$ -decay strength function. This model was used in many theoretical calculations of  $P_{xn}$  values, for example, the global calculation by Möller *et al.* [5], Marketin [6], or recently by Minato *et al.* [7]. In this approach, a strong dependence of delayed neutron emission on the decay strength distribution within a specific energy window is observed, leading to predictions of very strong multi-neutron emission channels for most exotic isotopes. However, this assumption may oversimplify the reality and competition between multi-neutron emission channels should be considered. By assuming sequential emissions of neutrons from a state above  $S_{2n}$  in the daughter nucleus, the final number of neutrons emitted in the the sequence depends on whether or not the first neutron took more energy than  $S_{2n} - S_{1n}$ . If the first emission populated a state below  $S_{1n}$ , two-neutron emission is no longer possible. Therefore, such competition could reduce multi-neutron emission probabilities from those predicted by the cutoff model assumption.

For nuclei with  $Q_\beta < S_{2n}$ ,  $\gamma$  emission from neutron-unbound states is the only competition that can reduce the neutron emission probability. The neutron- $\gamma$  competition was previously considered by experimentalists and theorists [8–12]. The significance of the relative competition between multi-neutron emission channels in the  $Q_\beta > S_{2n}$  nuclei was quantitatively discussed in the theoretical work by Mumpower *et al.* [13] and a modified

global prediction for neutron emission probabilities was provided using the QRPA strength distribution [14]. It was concluded that relative neutron emission branching ratios can affect the results of  $r$ -process nucleosynthesis models. However, the experimental data, which enable the evaluation of the competition between multi-neutron emission channels for the  $r$ -process nuclei are almost nonexistent. According to the Ref. [2], there are only a few two-neutron emitters and no three- or more-neutron emitters are known so far in nuclei with  $Z > 26$  which are relevant for  $r$ -process modeling.

$\beta$ -delayed two-neutron (2n) emission was first observed in 1979 [15] in  $^{11}\text{Li}$ . Unlike for one-neutron emitters, two-neutron emission probabilities ( $P_{2n}$ ) have been measured for fewer than ten nuclei heavier than iron. This is due to the challenges of producing sufficiently neutron-rich nuclei. Most identified 2n emitters are nuclei lighter than iron from Li to K [16–20]. For nuclei heavier than iron, there are known 2n emitters in  $^{98}\text{Rb}$  [21],  $^{100}\text{Rb}$  [22], and  $^{136}\text{Sb}$ [23] with small branching ratios of 0.060(9)%, 0.16(8)%, and 0.14(3)%, respectively. The first observation of strong two-neutron emission in the region relevant to the  $r$ -process was achieved for  $^{86}\text{Ga}$  with  $P_{2n} = 20(10)\%$  by Miernik *et al.* [24]. Other than that, the existence of a decaying branch to the two-neutron-emission daughter nuclei is confirmed by  $\beta$ - $\gamma$  spectroscopy without a neutron measurement in some nuclei, such as  $^{140}\text{Sb}$  [25] or  $^{134}\text{In}$  decay [26].

With the advent of radioactive ion beam facilities and efficient neutron detectors [27–30],  $\beta$ -delayed multi-neutron emitters are becoming accessible for study, and a number of papers on the new two-neutron measurements have recently been published [31–33]. The  $N > 50$  Ga isotopes are some of the best candidates to study multi-neutron emission heavier than iron since they are known to have strong neutron-emission branching ratios. This is due to their large energy window for  $\beta$  decay where most of the Gamow-Teller strength B(GT) is concentrated above neutron separation energies because of the  $N = 50$  shell gap [34]. Large  $P_{1n}$  values were measured for Ga isotopes, in  $^{83-86}\text{Ga}$  [24, 34–37].

In this work, we have measured the  $\beta$  decays of  $^{84-87}\text{Ga}$ .  $P_{1n}$  and  $P_{2n}$  values of these isotopes were reported previously in a Rapid Communication [31]. We have found large  $P_{1n}$  values and unexpectedly small  $P_{2n}$  values even for those Ga isotopes where the major part of the B(GT) is expected to be concentrated above  $S_{2n}$ . This was interpreted as a signature of one-neutron emission from two-neutron unbound states. These results confirmed experimentally for the first time that the assumption of the cutoff model is not valid when the two neutron emission channel is energetically available, and the competition between 2n and 1n emission processes has to be considered [31].

The  $\beta$ -delayed neutron emission is a two-step process, where the beta-decay strength distribution determines the first stage. The second stage has to consider the neutron-emission probability from excited nuclear states

---

\* yokoyama@cns.s.u-tokyo.ac.jp

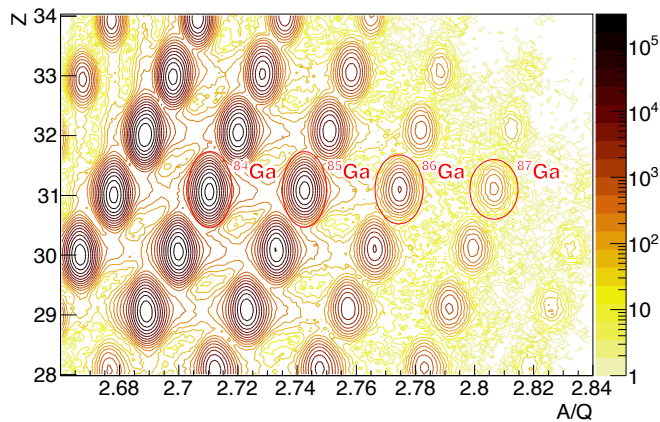


FIG. 1. Particle identification plot of the secondary beam at BigRIPS. The red ellipses indicate the gates applied to select each Ga ion. This plot shows the sum of the two different runs (see the text).

in  $\beta$ -decay daughter. The key questions for the modeling of the second phase of this process is the degree to which the nuclear structure affects neutron emission and how the details of this process should be modeled.

The work by Mumpower *et al.* [13] implements the strength function using QRPA and Hauser-Feshbach statistical model (QRPA-HF) for particle and  $\gamma$ -ray emissions [38]. This model calculates  $P_{1n}$  or  $P_{2n}$  by following statistical decays of both the delayed- $\gamma$  and neutron emission one by one until all the excitation energy is exhausted. The authors of Ref. [13] explored this framework and found only a slight improvement in branching ratios near stability but a substantial difference for neutron-rich nuclei closer to the drip line. This is due to the dominance of the multi-neutron emission processes in the very exotic nuclei that are typically involved in the  $r$ -process. The statistical model was then applied to the global calculation by Möller *et al.* [14] and the new  $P_{xn}$  predictions are in better agreement with our experimental data [31] compared to the ones using the cutoff model [5].

In this paper, we show a more detailed analysis of the  $P_{xn}$  values to narrow down the uncertainties that originated from the energy-dependent efficiency of the neutron detector and updated results from the previous paper, together with the new results from the  $\gamma$ -ray analysis. We also report a detailed analysis of the statistical model calculations using more realistic level densities from our experimental data and shell-model calculations, combined to discuss the sensitivity of the branching ratios to the nuclear structure in  $\beta$ -delayed neutron emission models.

## II. EXPERIMENTAL DETAILS

Neutron-rich Ga ( $Z = 31$ ) isotopes were studied by means of  $\beta$ -neutron- $\gamma$  spectroscopy at the RI Beam

Factory (RIBF) of the RIKEN Nishina Center. The neutron-rich nuclei were produced by in-flight fission of a 345 MeV/nucleon  $^{238}\text{U}^{86+}$  beam on a 4-mm thick  $^9\text{Be}$  production target. The measurements were performed in two independent runs with a slight  $B\rho$  (magnetic rigidity) difference. We call these runs run #1 and #2 in this paper. The typical intensity of the primary  $^{238}\text{U}$  beam was  $\approx 40$  pA and  $\approx 60$  pA for runs #1 and #2, respectively. Fission fragments were separated and identified in the BigRIPS in-flight separator [39] on an event-by-event basis by their proton numbers ( $Z$ ) and the mass-to-charge ratio ( $A/Q$ ). These quantities were obtained by measuring  $B\rho$ , the time-of-flight (TOF), and energy loss ( $\Delta E$ ) in BigRIPS. The TOF was obtained from the time difference between plastic scintillation counters at the achromatic foci F3 and F7. The  $B\rho$  values were obtained by ion trajectory reconstruction using position and angular information measured by position-sensitive parallel-plate avalanche counters (PPACs) [40]. The atomic number was obtained by measuring the energy loss ( $\Delta E$ ) in an ionization chamber [41] at the F7 focal plane. A detailed explanation of the particle identification at BigRIPS is found in Ref. [42, 43]. The particle identification plot is shown in Fig.1. There were  $9 \times 10^6$ ,  $3 \times 10^6$ ,  $7 \times 10^4$ , and  $6 \times 10^3$   $^{84-87}\text{Ga}$  ions implanted in total in the two runs, respectively.

The secondary beam was transported to the F11 focal plane and implanted into active stoppers made of double-sided silicon-strip detectors (DSSDs) for ion and  $\beta$  correlation. The AIDA (Advanced Implantation Detector Array) [44] was used in the run #1 whereas WAS3ABi [45] was employed for the run #2. A YSO scintillation detector [46] was also installed as a stopper for lighter mass ions than Ni. AIDA is a stack of 6 layers of DSSDs whose wafer has a thickness of 1 mm and is segmented into 128 strips with 0.560 mm pitch in both  $x$  and  $y$  directions.  $\beta$  particles detected within a 1.96-mm (3.5 strip width) radius of an implanted ion were correlated. WAS3ABi has four layers of DSSDs with 16 3-mm strips for  $x$  and  $y$ . The ion- $\beta$  correlation was made by a 3-mm (1 strip width) distance. The typical rate of the ion implantation in AIDA during the run #1 was  $\approx 150$  cps in total, whereas that in WAS3ABi during the run #2 was  $\approx 60$  cps. Among all the ions implanted in the DSSD arrays, about 18% were  $^{84}\text{Ga}$ .

The active stopper detector was placed in the center of a high-density polyethylene moderator of BRIKEN [30, 48, 49]. The BRIKEN system is composed of 140 proportional counters filled with  $^3\text{He}$  gas for neutron detection and two clover-type high-purity Ge detectors from the CLARION array of Oak Ridge National Laboratory [50] for high-resolution  $\gamma$ -ray detection. In this configuration, BRIKEN has 62(2)% neutron efficiency ( $\epsilon_n$ ) at  $\approx 1$  MeV neutron energy [30].

The photo-peak efficiency of the two clover detectors for 1 MeV gamma rays is  $\approx 3.5\%$  for a point source at the center of the array. Since the implantation distribution in each layer of the detectors is different for each nuclide,

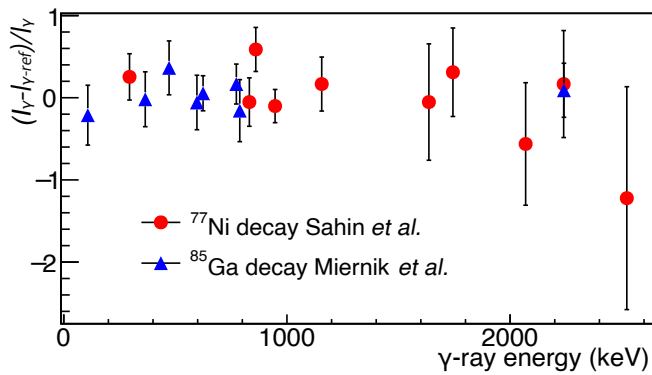


FIG. 2. Comparison of the  $\gamma$ -ray intensities between this work ( $I_\gamma$ ) and previous studies ( $I_{\gamma-ref}$ ). The red circle shows the  $\gamma$  rays in the decay of  $^{77}\text{Cu}$  previously reported by Sahin *et al.* [47] and the blue triangles are the ones from  $^{85}\text{Ga}$  decay by Miernik *et al.* [36].

Monte Carlo simulations by GEANT4 were performed to estimate nuclide-by-nuclide efficiencies using the experimental implantation profiles. The systematic error in the efficiencies from the geometrical uncertainties in the experimental setup was estimated as 4% by changing the clover position in the simulation by 2 mm which is the maximum uncertainty expected from the geometrical precision of the detector setup. The  $\gamma$ -ray intensities in the decay of  $^{77}\text{Ni}$  and  $^{85}\text{Ga}$  are compared with previous studies [36, 47] as shown in Fig. 2. Our  $\gamma$ -intensity analysis is consistent with previous work in the energy range of  $\approx 100$  keV and  $\approx 2$  MeV.

### III. RESULTS

#### A. $P_{xn}$ VALUES

The neutron-gated ion- $\beta$  time spectra for  $^{84}\text{Ga}$  and  $^{85}\text{Ga}$  decays obtained in the run #2 are presented in Fig.3. The same plots for  $^{86}\text{Ga}$  and  $^{87}\text{Ga}$  were shown in the previous publication [31]. Neutron events were correlated with a  $\beta$ -decay event if it was in a 200  $\mu\text{s}$  time window after the  $\beta$ -ray emission. The half-lives ( $T_{1/2}$ ) and initial decay rates at  $T_\beta - T_{ion} = 0$  for each neutron multiplicity ( $A_{0n}, A_{1n}$ , and  $A_{2n}$ ) were obtained by binned maximum likelihood fitting to a function with the decays of parent, daughter, 1n-daughter, and 2n-daughter, as well as a linear background. The half-lives of the daughter nuclei,  $^{84}\text{Ge}$ ,  $^{85}\text{Ge}$ , were fixed to the literature values, 942 ms, and 494 ms, respectively [51]. Short fitting ranges from 6 ms to 510 ms for  $^{84}\text{Ga}$  and 550 ms for  $^{85}\text{Ga}$  ( $\approx 6 \times T_{1/2}$ ) were employed in order to minimize uncertainty coming from descendant decays. In the 1n and 2n spectra, the portion of the parent decay is larger than those of 0n decays because the descendant nuclei are less exotic and have lower  $P_n$  values. Half-lives of 1n spectra are chosen as the reported values since the 1n spectra

had a smaller component from descendant nuclei than 0n spectra and higher statistics than those of 2n decays.

In the fitting of 0n and 2n spectra, the half-lives of parent nuclei were fixed to the values obtained from 1n spectra. Since the neutron efficiency is not 100%,  $A_{0n}$  includes 1n or 2n events with undetected neutrons. Also,  $A_{1n}$  and  $A_{2n}$  includes 0n or 1n events in coincidence with random background neutrons. A conversion matrix from  $P_{xn}$  to  $A_{xn}$ ,  $E$  is defined as

$$\begin{pmatrix} A_{0n} \\ A_{1n} \\ A_{2n} \end{pmatrix} = E \begin{pmatrix} P_{0n} \\ P_{1n} \\ P_{2n} \end{pmatrix} \quad (1)$$

as shown in Ref. [49]. The  $P_{xn}$  values are derived from  $A_{xn}$  values by calculating the inverse matrix,  $E^{-1}$ . The random neutron coincidence probabilities,  $r_{xn}$ , in the matrix shown as Eq. 2 of the Ref. [49], were estimated from the spectra of nuclei with  $Q_\beta < S_{2n}$ . The probabilities of having one background neutron in the 200  $\mu\text{s}$  correlation time window over no neutron are estimated to be  $r_{1n}/r_{0n} = 0.010$  and 0.012 for runs #1 and #2, respectively. We assumed that the random neutrons are independent of each other, providing the following relationship,  $r_{2n} = r_{1n}^2$ . The half-lives and branching ratios were obtained separately for each of the two runs since the  $r_{1n}$  values are slightly different due to the beam rate, degrader thickness, and implant detector setups. The  $T_{1/2}$  and  $P_{xn}$  values obtained for each run, and the average of the two are summarized in TABLE. I. Details of the general analysis for obtaining  $P_{xn}$  values are described in [49].

Although the BRIKEN array has minimized energy dependency of the neutron detection efficiency up to a few MeV, the efficiency still drops at a few MeV or higher, due to its large high-density polyethylene moderator. The neutron efficiency varies from 50 % for 5 MeV to 68 % for low-energy neutrons, as shown in the yellow dashed curve in Fig. 4, and therefore, We need to make an assumption of the neutron spectrum unless it is measured experimentally. In the previous paper [31], we reported  $P_{xn}$  values with larger uncertainties by using shell-model-generated neutron spectra. These spectra provide a lower limit on the neutron efficiency since it assumes that all the excitation energies are taken out by neutrons but not by  $\gamma$  rays. In the current work, we applied the statistical model calculation described later in Sec. IV, to narrow down the neutron efficiency by convoluting the calculated energy spectra and the simulated efficiency curve as shown in Fig. 4. For the systematic errors, the neutron efficiencies were varied by shifting the GT strength 500 keV in the statistical model calculations. The  $P_{xn}$  values are reported in Table. I. The obtained values have smaller systematic errors than those reported in the previous paper [31]. The dataset of run #1 was analyzed before, and the  $P_{xn}$  and  $T_{1/2}$  values are summarized in [52]. There are minor differences between values presented in those previous works and this paper owing to updated neutron efficiency analysis.

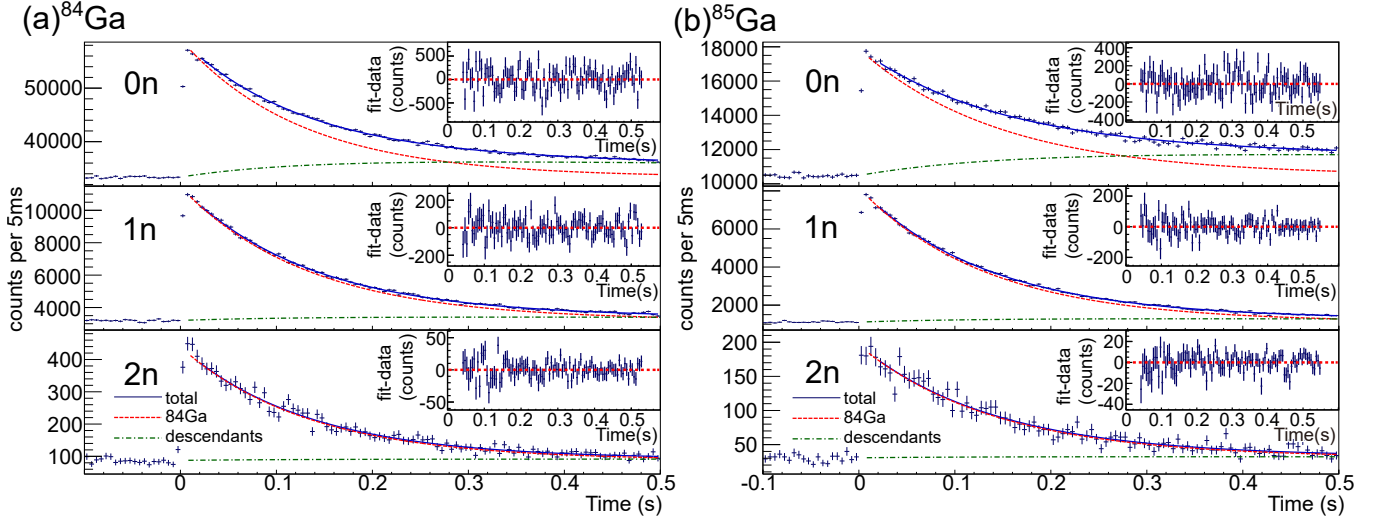


FIG. 3. The decay curves gated by neutron multiplicity 0, 1, and 2 for (a)  $^{84}\text{Ga}$  and (b)  $^{85}\text{Ga}$ . The solid blue curves represent the fitting functions. The dashed red curves show the decay components of the precursor nuclei. The dashed-dotted green curves are the sum of the daughter decays, including neutron emission branches. The plots at the top right corners of each spectrum are the residuals of the decay spectra from the fitting function.

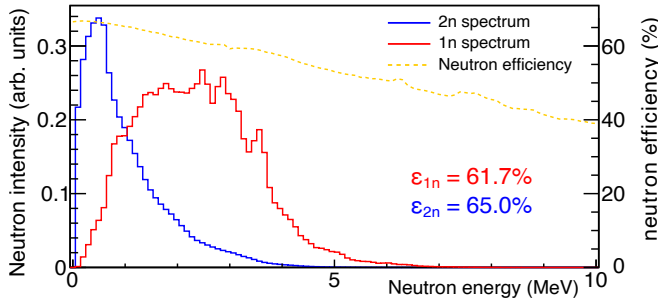


FIG. 4. Neutron energy spectra expected in the decay of  $^{86}\text{Ga}$  predicted from the statistical model calculation using  $B(GT)$  predicted by the shell model [34]. The red and blue histograms show the single-neutron energy spectra for 1n and 2n channels, respectively. The dashed orange curve shows the simulated neutron detection efficiency of the BRIKEN array [30] whose axis is on the right-hand side of the plot.

### B. n- $\beta$ - $\gamma$ ANALYSIS

In the following subsections,  $\beta$ -neutron gated  $\gamma$  spectra for the decay of  $^{84-87}\text{Ga}$  are shown. The  $\gamma$  rays following  $\beta$  decays were correlated with a  $7 \mu\text{s}$  time window. The  $\gamma$ -ray intensities per precursor decay ( $I_\gamma$ ) are deduced from the  $\gamma$ -ray peak area and the number of  $\beta$  events ( $N_\beta$ ) that were used to generate the  $\gamma$ -ray spectrum.  $I_\gamma$  is defined as,

$$I_\gamma = A_{peak}/(\varepsilon_\gamma \varepsilon_{xn} N_\beta) \quad (2)$$

where  $\varepsilon_\gamma$  and  $\varepsilon_{xn}$  are the  $\gamma$ -ray and  $x$ -neutron detection efficiencies by simulations.  $N_\beta$  is the integral of the positive part of the time spectrum up to the time window ( $t_w$ ), subtracted by the negative part as a random

TABLE I. Half-lives,  $P_{1n}$ , and  $P_{2n}$  obtained in this study. Values from the two different runs and their weighted averages (adop.) are shown.

nuclide	$T_{1/2}$ (ms)	branching ratio (%)	
		$P_{1n}$	$P_{2n}$
$^{84}\text{Ga}$ run #1	95.0(25)	38.2(21)*	1.91(17)*
$^{84}\text{Ga}$ run #2	97.6(12)	37.0(4)*	1.87(7)*
$^{84}\text{Ga}$ adop.	97.1(11)	37.0(4)*(11) <sup>†</sup>	1.88(6)*(11) <sup>†</sup>
$^{85}\text{Ga}$ run #1	101(4)	73(4)*	1.8(3)*
$^{85}\text{Ga}$ run #2	95.3(10)	76.4(18)*	1.53(14)*
$^{85}\text{Ga}$ adop.	95.6(10)	75.8(18)*(24) <sup>†</sup>	1.58(13)*(9) <sup>†</sup>
$^{86}\text{Ga}$ run #1	53(4)	57(6)*	17.8(22)*
$^{86}\text{Ga}$ run #2	51(2)	59.9(23)*	14.1(10)*
$^{86}\text{Ga}$ adop.	51(2)	59.5(21)*(18) <sup>†</sup>	14.7(9)*(11) <sup>†</sup>
$^{87}\text{Ga}$ run #1	31(9)	73(31)*	18(18)*
$^{87}\text{Ga}$ run #2	24(8)	72(9)*	8.5(28)*
$^{87}\text{Ga}$ adop.	27(6)	72(9)*(2) <sup>†</sup>	8.7(28)*(5) <sup>†</sup>

\*statistical errors, <sup>†</sup>systematic errors

$\beta$ -implant correlations:

$$N_\beta = r_{precursor} \left( \int_0^{t_w} N_{tot}(t) dt - \int_{-t_w}^0 N_{tot}(t) dt \right) \quad (3)$$

Ratio of the precursor activity in the total Bateman function ( $r_{precursor}$ ) is calculated as follows.

$$r_{precursor} = \frac{A_0}{A_0 + A_1 + \dots}$$

$$A_0 = \int_0^{t_w} e^{-\lambda_0 t} dt$$

$$A_1 = \int_0^{t_w} \frac{\lambda_1}{\lambda_1 - \lambda_0} (e^{-\lambda_0 t} - e^{-\lambda_1 t}) dt$$
(4)

$A_0, A_1, \dots$  and  $\lambda_0, \lambda_1, \dots$  are the activities and decay rates of precursor (0) and descendant (1,2,...) nuclides.

### 1. $^{84}\text{Ga}$

Delayed-neutron emission in the decay of  $^{84}\text{Ga}$  was previously measured by using proton-induced fission of  $^{238}\text{U}$  at HRIBF, ORNL [35], photo-fission of uranium target at ALTO, IPN Orsay [37, 53], and ISOLDE at CERN [34]. The reported  $P_{1n}$  values by those previous works are 74(14) % [54], 53(20) % [37], and 40(7) % [34], respectively. The adopted value from this work is 37.0(12) % which supports the last two values. The adopted half-life of  $^{84}\text{Ga}$  from this work, 97.1(11) ms is consistent with the value reported before, 85(10) ms [55].

TABLE II. List of  $\gamma$  rays observed in the decay of  $^{84}\text{Ga}$ .  $I_\gamma$  is the number of  $\gamma$  rays emitted per 100  $^{84}\text{Ga}$  decays.

$E_\gamma$ (keV)	$I_\gamma$ (%)	$T_{1/2}$ (ms)	decay channel
624.10(4)*(38) <sup>†</sup>	6.4(2)*(4) <sup>†</sup>	91(5)	$\beta$
1604.1(3)*(4) <sup>†</sup>	0.69(18)*(4) <sup>†</sup>	-	$\beta$
2877.7(3)*(4) <sup>†</sup>	1.27(25)*(8) <sup>†</sup>	-	$\beta$
3501.93(14)*(38) <sup>†</sup>	5.3(3)*(3) <sup>†</sup>	101(11)	$\beta$
247.58(20)*(38) <sup>†</sup>	11.3(2)*(7) <sup>†</sup>	88(2)	$\beta n$
798.97(35)*(38) <sup>†</sup>	0.46(9)*(3) <sup>†</sup>	-	$\beta n$
941.1(3)*(4) <sup>†</sup>	1.01(11)*(6) <sup>†</sup>	-	$\beta n$
1045.93(9)*(38) <sup>†</sup>	7.4(3)*(4) <sup>†</sup>	91(4)	$\beta n$
1204.3(5)*(4) <sup>†</sup>	0.70(11)*(4) <sup>†</sup>	-	$\beta n$
1239.38(21)*(38) <sup>†</sup>	0.76(11)*(5) <sup>†</sup>	-	$\beta n$
1794.80(19)*(38) <sup>†</sup>	2.19(24)*(13) <sup>†</sup>	-	$\beta n^\ddagger$
1969.4(5)*(4) <sup>†</sup>	0.78(13)*(8) <sup>†</sup>	107(13)	$\beta n^\ddagger$
2112.6(3)*(4) <sup>†</sup>	0.33(8)*(2) <sup>†</sup>	108(18)	$\beta n$
2910.7(4)*(4) <sup>†</sup>	0.20(6)*(2) <sup>†</sup>	85(20)	$\beta n$
217.3(5)*(4) <sup>†</sup>	0.028(12)*(2) <sup>†</sup>	-	$\beta 2n^\ddagger$
1348.3(4)*(4) <sup>†</sup>	0.47(9)*(3) <sup>†</sup>	50(12)	$\beta 2n$

\*statistical errors, <sup>†</sup>systematic errors, <sup>‡</sup>not assigned

Figure 5 shows the  $\gamma$ -ray energy spectra in the decay of  $^{84}\text{Ga}$  gated by the neutron multiplicities. There is a clear peak at 1348 keV in the 2n gated spectrum in the figure which is interpreted as  $2^+ \rightarrow 0^+$  of  $^{82}\text{Ga}$  in the  $\beta_{2n}$  branch. In the previous work [37], there is a candidate at this energy in  $\beta$ -n gated  $\gamma$  spectrum with very limited

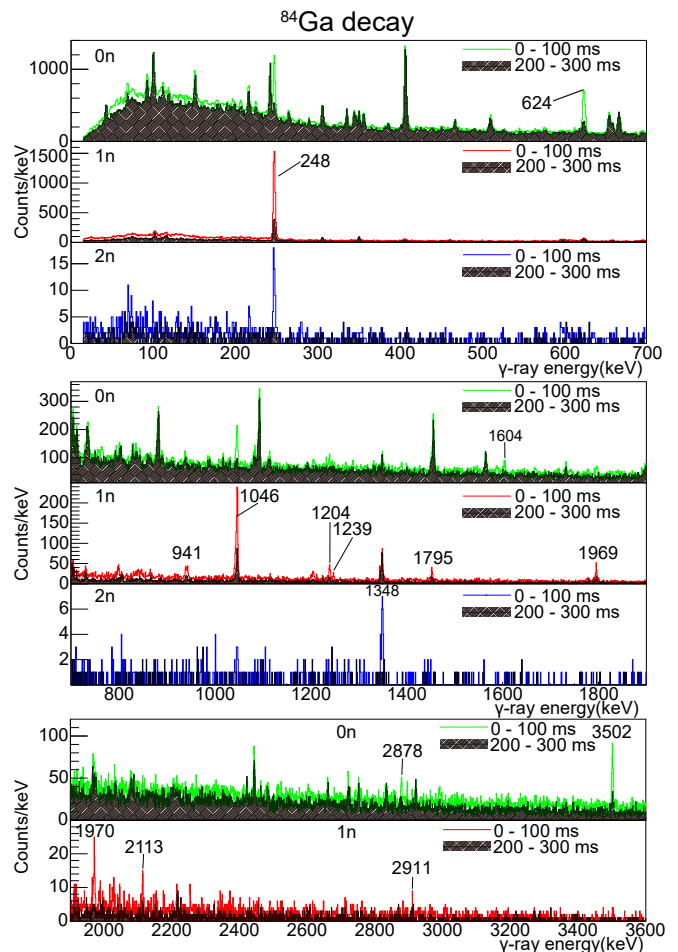


FIG. 5. Gamma-ray energy spectra of  $^{84}\text{Ga}$  gated by neutron multiplicities. Green, red, and blue histograms show  $\gamma$  rays observed with the neutron multiplicity equal to 0, 1, and 2, respectively. Histograms with a time window from 0 to 100 ms are drawn in lighter colors while the ones from 200 to 300 ms are drawn in darker colors and hatched in order to distinguish if the peaks originate in the parent  $^{84}\text{Ga}$  decay or from the decay of the descendant nuclei. Peaks that are distinct only in the lighter colors are regarded as the  $\gamma$  rays from the decay of  $^{84}\text{Ga}$ .

statistics. The  $\gamma$ -ray energies and intensities measured in this work are summarized in Table II.

Figure 6 shows the decay scheme of  $^{84}\text{Ga}$  obtained in this work. This scheme is consistent with the reported one [53] except for the 2113-keV line, which has not been reported in the literature.

### 2. $^{85}\text{Ga}$

The  $\beta$ - $\gamma$  spectrum of  $^{85}\text{Ga}$  was previously measured by Korgul *et al.* [59] and then by Miernik *et al.* [36] including the  $\beta$ -n- $\gamma$  spectrum. We observed the  $\beta$ -n-n- $\gamma$  spectrum for the first time as shown in Fig. 7. There is a clear peak at 247 keV in the spectrum, which is at

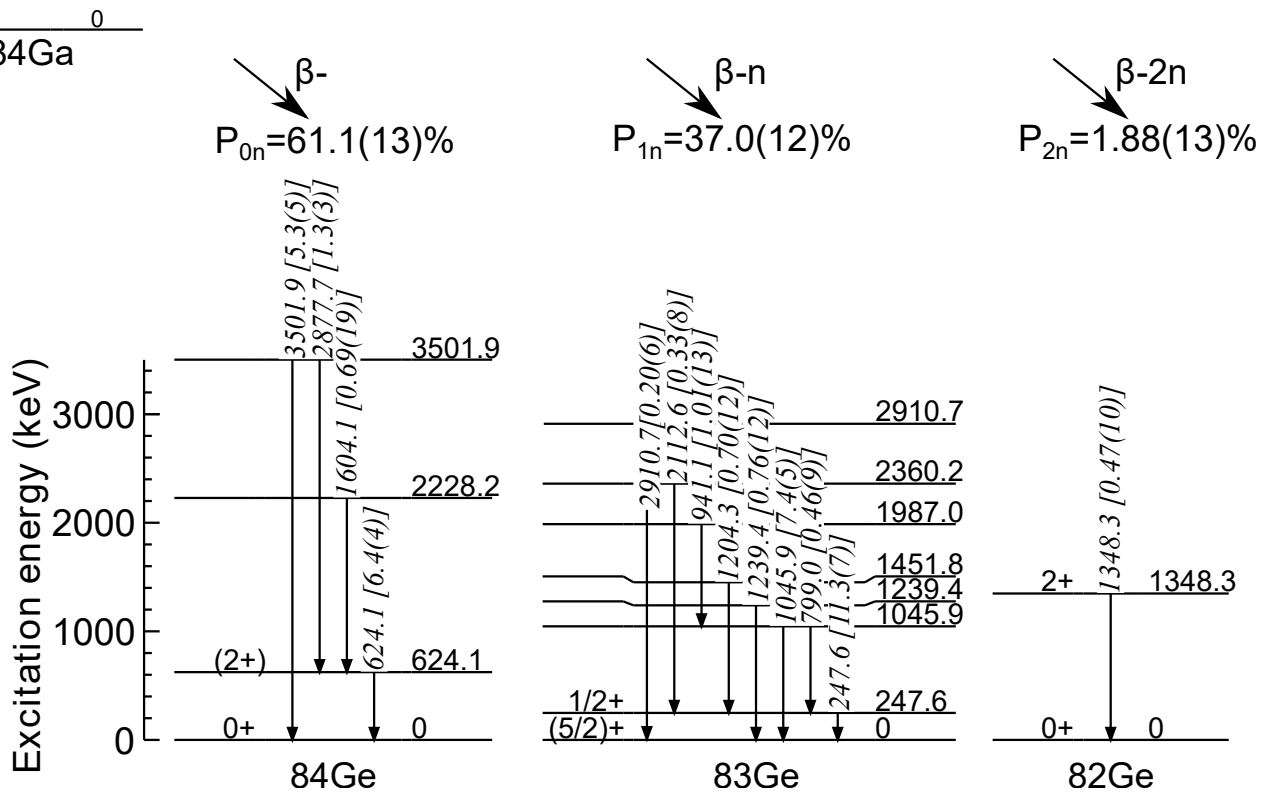


FIG. 6. Level scheme of  $^{82-84}\text{Ge}$  populated in the  $\beta$  decays of  $^{84}\text{Ga}$ . Spin-parity assignments are from Refs. [56–58]. Intensities of the  $\gamma$  transitions in square parentheses are given per 100  $^{84}\text{Ga}$  decays.

the same energy as the  $1/2_1^+ \rightarrow g.s.$   $\gamma$ -ray in  $^{83}\text{Ga}$  [54]. This result shows that there is two-neutron branching in the decay of  $^{85}\text{Ga}$ , which is consistent with the branching ratio obtained by the neutron detector, 1.6(2)%. The reported upper limit of the  $P_{2n}$  value by Miernik *et al.* was  $<0.1\%$ . The observed coincidence between two neutrons and the 247-keV  $\gamma$ -ray supports that our  $P_{2n}$  value is more reliable. The discrepancy may be attributed to differences in detection energy thresholds for  $\beta$  particles.

Levels of the daughter Ge nuclei constructed from this work are shown in Fig. 8. The levels in the  $^{85}\text{Ge}$  nuclei are consistent with previous measurement [36, 59]. Ref. [59] assigned 773-keV peak to the decay of  $^{84}\text{As}$ . We observed, however, a 78(12) ms decay curve for this peak which supports the assignment of Ref. [36] as a transition in  $^{85}\text{Ge}$ . As in Ref. [36] it assigned to a level at 773 keV since there was no coincidence observed with any other  $\gamma$  lines in  $^{85}\text{Ge}$ . We observed 596-keV transition which was not reported in Ref. [36] but in Ref. [59]. The 859-keV transition is assigned above the 1430-keV state since  $\gamma$ - $\gamma$  coincidences are observed between the 806-keV and 624-keV transitions, as shown in Fig. 7. In addition, a new  $\gamma$  line at 1893 keV is observed and tentatively assigned as the decay from the new state at 3281 keV to the 1389-keV state because there is only one 1892-keV  $\gamma$  event recorded in coincidence with the 765-keV one, which is not sufficient to unambiguously assign the placement of

the state.

### 3. $^{86}\text{Ga}$

The decay of the  $^{86}\text{Ga}$  nucleus was previously reported by Miernik *et al.* [24]. The  $P_{xn}$  values from their work,  $P_{1n} = 60(10)\%$ ,  $P_{2n} = 20(10)\%$  are consistent with our values,  $P_{1n} = 60(3)\%$ ,  $P_{2n} = 14.7(14)\%$ .  $\beta$ - $\gamma$  spectra with neutron multiplicity gates are shown in Fig. 9 and the energies and intensities of the  $\gamma$  peaks are summarized in Table IV. We observed the 624-keV  $\gamma$  ray from the two-neutron decay channel that was reported in the previous study [24] but with two-neutron coincidences. We also observed  $\gamma$  rays from one-neutron decays reported in Ref. [24], in addition to the 472- and 773-keV transitions which were previously known in the zero-neutron decay of  $^{85}\text{Ga}$  [36]. A  $\gamma$ -ray peak at 1024 keV was observed in the zero-neutron emission channel. The half-life of the  $\gamma$  peak, 61(15) ms is consistent with the adopted decay half-life, 52(2). Since there were no  $\gamma$ - $\gamma$  coincidence events observed, it was tentatively assigned to a new state in  $^{86}\text{Ge}$  at 1024 keV, a candidate for the second  $2^+$  state as reported by Ref. [56] at 1046(14).

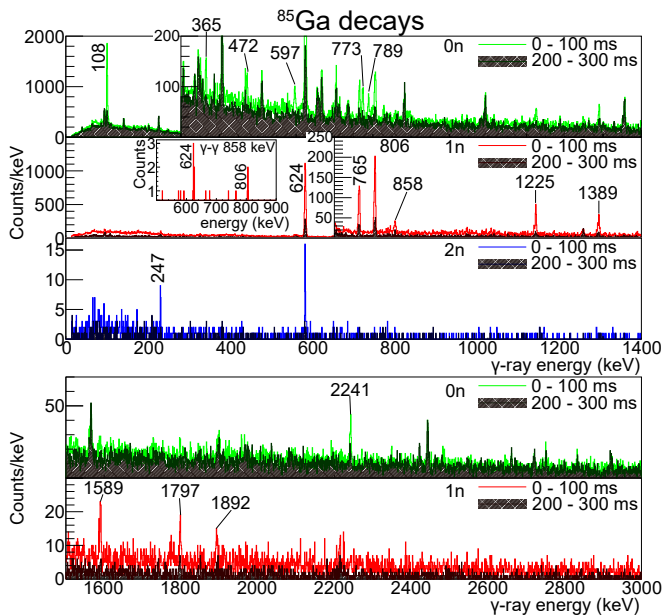


FIG. 7. Gamma-ray energy spectra of  $^{85}\text{Ga}$  gated by neutron multiplicities. See the caption of 5 for details. A part of the  $\gamma$ - $\gamma$  coincidence spectrum gated by the 858-keV peak is shown in the 1n spectrum in the upper panel.

#### 4. $^{87}\text{Ga}$

The decay of  $^{87}\text{Ga}$  had not been measured before. The  $\gamma$ -ray spectra and the list of the peaks are shown in Fig. 11 and Table V, respectively. The  $(2^+) \rightarrow 0^+$  transition in  $^{86}\text{Ge}$  at 527 keV and the 108-keV transition in  $^{85}\text{Ga}$  are observed in the decay of  $^{87}\text{Ga}$  for the first time. The 786.1-keV peak in the 1n spectrum could be the 791(23) transition from the  $(4_1^+)$  level in  $^{86}\text{Ga}$  proposed by the Ref. [56] using in-flight  $\gamma$ -ray spectroscopy of (p, 2p) reaction.

#### C. ISOMERIC TRANSITION IN $^{86}\text{Ga}$

A delayed  $\gamma$ -ray peak was observed at 97.8(4) keV after the implantation of  $^{86}\text{Ga}$  as shown in Fig. 12. The half-life of this isomeric state was observed to be 0.32(3)  $\mu\text{s}$ . The ground-state spin and parity ( $J^\pi$ ) of the odd-odd  $^{86}_{31}\text{Ga}_{55}$  nucleus is not known, and no excited states have ever been measured before. There is an isomer known in  $^{92}_{37}\text{Rb}_{55}$  at 284.2 keV with half-life of 54(3) ns [62]. This isomer decays by 142-keV  $E2$  transition with  $B(E2) = 7.2(4)$  W.u. which is typical for spherical nuclei around the  $Z = 36$ -40 region [62]. The new isomeric decay in  $^{86}\text{Ga}$  has  $B(E2) = 5.0(5)$  W.u. using the internal conversion coefficient from BrIcc [63] assuming an  $E2$  transition. This is a reasonable value for spherical nuclei as in the case of  $^{92}\text{Rb}$  [62], and not contradicting various global calculations [64, 65] predicting  $^{86}\text{Ga}$  to be nearly spherical.

TABLE III. List of  $\gamma$  rays observed in the decay of  $^{85}\text{Ga}$ .  $I_\gamma$  is the number of  $\gamma$  rays emitted per 100  $^{85}\text{Ga}$  decays.

$E_\gamma$ (keV)	$I_\gamma$ (%)	$T_{1/2}$ (ms)	decay channel
107.83(2)*(38) <sup>†</sup>	9.9(3)*(6) <sup>†</sup>	89(2)	$\beta$
365.15(16)*(38) <sup>†</sup>	1.09(16)*(7) <sup>†</sup>	107(16)	$\beta$
471.89(23)*(38) <sup>†</sup>	1.10(27)*(7) <sup>†</sup>	-	$\beta$
596.66(28)*(38) <sup>†</sup>	1.04(17)*(6) <sup>†</sup>	89(20)	$\beta$
704.20(17)*(38) <sup>†</sup>	1.64(20)*(10) <sup>†</sup>	-	$\beta$
773.30(17)*(38) <sup>†</sup>	2.46(27)*(15) <sup>†</sup>	84(11)	$\beta$
788.65(26)*(38) <sup>†</sup>	1.21(22)*(7) <sup>†</sup>	106(23)	$\beta$
2241.03(27)*(38) <sup>†</sup>	1.65(21)*(10) <sup>†</sup>	83(23)	$\beta$
624.18(27)*(38) <sup>†</sup>	42.3(11)*(25) <sup>†</sup>	92.5(17)	$\beta\text{n}$
765.02(9)*(38) <sup>†</sup>	6.0(3)*(7) <sup>†</sup>	89(7)	$\beta\text{n}$
806.06(8)*(38) <sup>†</sup>	8.6(15)*(5) <sup>†</sup>	92(4)	$\beta\text{n}$
858.5(4)*(4) <sup>†</sup>	1.47(25)*(17) <sup>†</sup>	-	$\beta\text{n}$
1225.08(14)*(38) <sup>†</sup>	3.02(23)*(18) <sup>†</sup>	96(6)	$\beta\text{n}$
1388.61(21)*(38) <sup>†</sup>	4.03(30)*(24) <sup>†</sup>	90(13)	$\beta\text{n}$
1588.9(4)*(4) <sup>†</sup>	1.53(25)*(17) <sup>†</sup>	100(13)	$\beta\text{n}^\ddagger$
1797.3(4)*(4) <sup>†</sup>	0.99(22)*(11) <sup>†</sup>	85(12)	$\beta\text{n}$
1893.0(5)*(4) <sup>†</sup>	0.91(25)*(11) <sup>†</sup>	83(11)	$\beta\text{n}$
3359.3(5)*(4) <sup>†</sup>	0.29(13)*(3) <sup>†</sup>	75(27)	$\beta\text{n}^\ddagger$
247.3(3)*(4) <sup>†</sup>	0.12(4)*(1) <sup>†</sup>	-	$\beta 2\text{n}$

\*statistical errors, <sup>†</sup>systematic errors, <sup>‡</sup>not assigned

TABLE IV. List of  $\gamma$  rays observed in the decay of  $^{86}\text{Ga}$ .  $I_\gamma$  is the number of  $\gamma$  rays emitted per 100  $^{86}\text{Ga}$  decays.

$E_\gamma$ (keV)	$I_\gamma$ (%)	$T_{1/2}$ (ms)	decay channel
527.30(21)*(38) <sup>†</sup>	7.3(8)*(4) <sup>†</sup>	60(8)	$\beta$
1024.3(9)*(4) <sup>†</sup>	2.8(9)*(2) <sup>†</sup>	-	$\beta$
107.87(8)*(38) <sup>†</sup>	13.3(9)*(8) <sup>†</sup>	48(3)	$\beta\text{n}$
249.94(14)*(38) <sup>†</sup>	7.6(7)*(7) <sup>†</sup>	47(5)	$\beta\text{n}$
365.04(15)*(38) <sup>†</sup>	3.9(6)*(2) <sup>†</sup>	66(9)	$\beta\text{n}$
472.9(3)*(4) <sup>†</sup>	3.2(7)*(4) <sup>†</sup>	57(10)	$\beta\text{n}$
773.5(4)*(4) <sup>†</sup>	2.8(8)*(2) <sup>†</sup>	-	$\beta\text{n}$
623.89(18)*(38) <sup>†</sup>	5.5(11)*(5) <sup>†</sup>	-	$\beta 2\text{n}$

\*statistical errors, <sup>†</sup>systematic errors

We performed shell-model calculations with jj45pna [66] using KSHELL [67] code. It predicts the ground-state  $J^\pi = 3^+$  for  $^{86}\text{Ga}$  and a  $5^+$  state at 98 keV which is decaying by an  $E2$  transition with 14.6 W.u. strength. On the other hand, NuShellX calculations predict two possibilities for low-lying isomeric transitions, one with  $7^+$  and  $5^+$  pair and another with  $2^-$  and  $0^-$  pair with  $B(E2)$  between 5 and 10 W.u. In both calculations, the configurations of the low-lying states are very fragmented between involved proton and neutron orbitals.



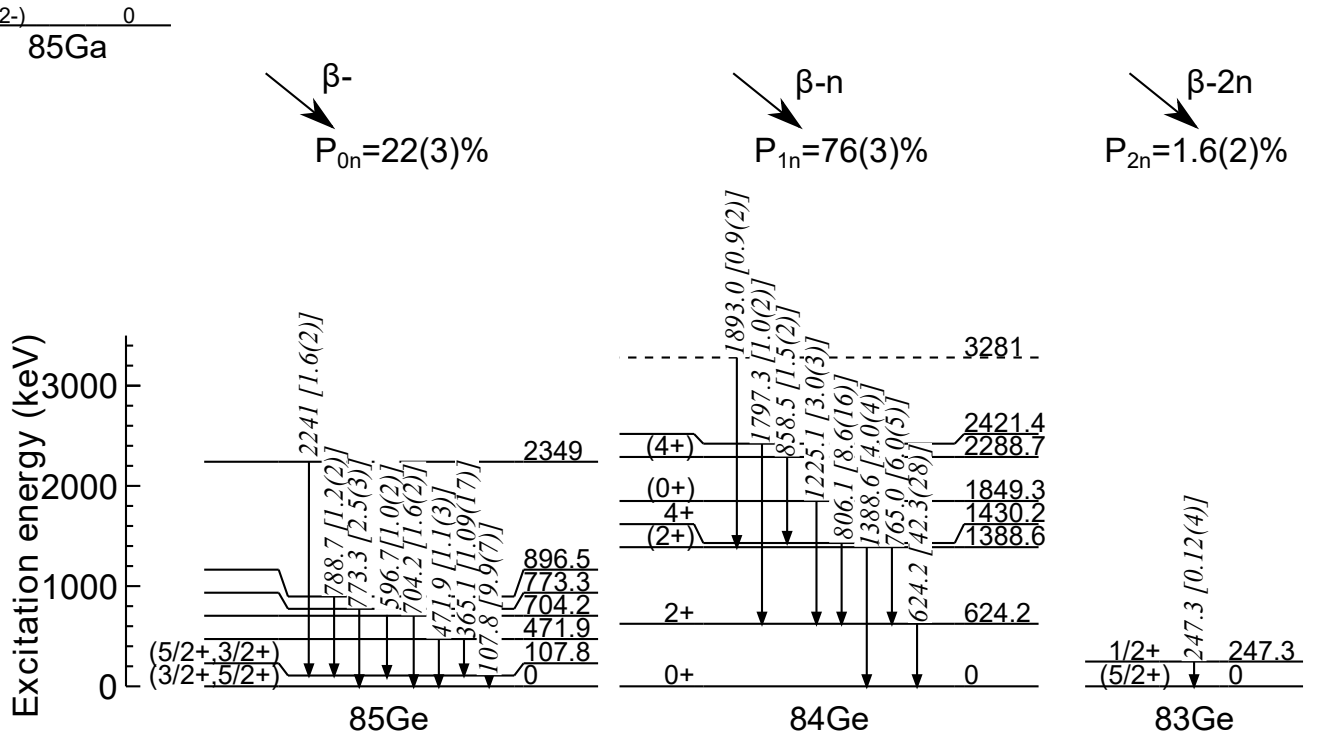


FIG. 8. Level scheme of  $^{83-85}\text{Ge}$  populated in the  $\beta$  decays of  $^{85}\text{Ga}$ . Spin-parity assignments are from Refs. [56, 57, 60]. Intensities of the  $\gamma$  transitions in square parentheses are given per 100  $^{85}\text{Ga}$  decays.

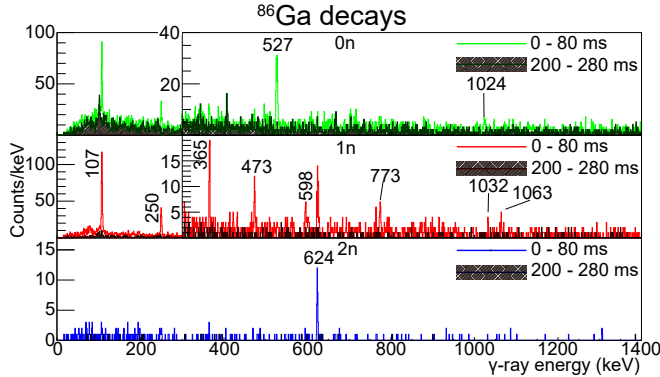


FIG. 9. Gamma-ray energy spectra of  $^{86}\text{Ga}$  gated by neutron multiplicities.

#### IV. DISCUSSION

The neutron energy spectra in the decay of  $^{83,84}\text{Ga}$  were previously measured by Madurga *et al.* [34]. Observation of high-energy neutrons emitted after beta decay was interpreted as a signature of the shell structure effects that dominate the beta-decay process. In their work, a comparison between existing data and experiments was made for lifetimes and branching ratios, based on the determination of the details of the strength distribution, but no statistical model treatment was included to make predictions of  $P_{xn}$ .

TABLE V. List of  $\gamma$  rays observed in the decay of  $^{87}\text{Ga}$ .  $I_\gamma$  is the number of  $\gamma$  rays emitted per 100  $^{87}\text{Ga}$  decays.

$E_\gamma$ (keV)	$I_\gamma$ (%)	$T_{1/2}$ (ms)	decay channel
1712.6(7)*(4) <sup>†</sup>	6.9(34)*(4) <sup>†</sup>	-	$\beta^\ddagger$
2661.9(9)*(4) <sup>†</sup>	6.5(43)*(4) <sup>†</sup>	-	$\beta^\ddagger$
178.2(6)*(4) <sup>†</sup>	5.1(29)*(6) <sup>†</sup>	-	$\beta n^\ddagger$
527.2(3)*(4) <sup>†</sup>	58(10)*(6) <sup>†</sup>	27(8)	$\beta n$
786.1(3)*(4) <sup>†</sup>	7.9(36)*(9) <sup>†</sup>	-	$\beta n$
108.4(5)*(4) <sup>†</sup>	10.9(45)*(10) <sup>†</sup>	-	$\beta 2n$

\*statistical errors, <sup>†</sup>systematic errors, <sup>‡</sup>not assigned

As discussed in the previous letter [31], there is a discrepancy in the  $P_{1n}$  and  $P_{2n}$  values of  $^{87}\text{Ga}$  between the experimental and the predicted values by Madurga *et al.* [34]. We applied the Hauser-Feshbach statistical model [38] to the shell-model calculation based on the work by Madurga [34] and the discrepancy was interpreted as one-neutron emission from two-neutron unbound states in the daughter nuclei. In this paper, we will describe more details of the shell model and the statistical model and will discuss the effect of level densities in daughter nuclei on the  $P_{xn}$  values by the statistical model calculation.

The model for the GT decay strength distribution for Ga isotopes [34] was based on a shell-model calculation for the  $\beta$  decay of Ga isotopes using the NuShellX code [68] with hybrid interactions and the truncation as pre-

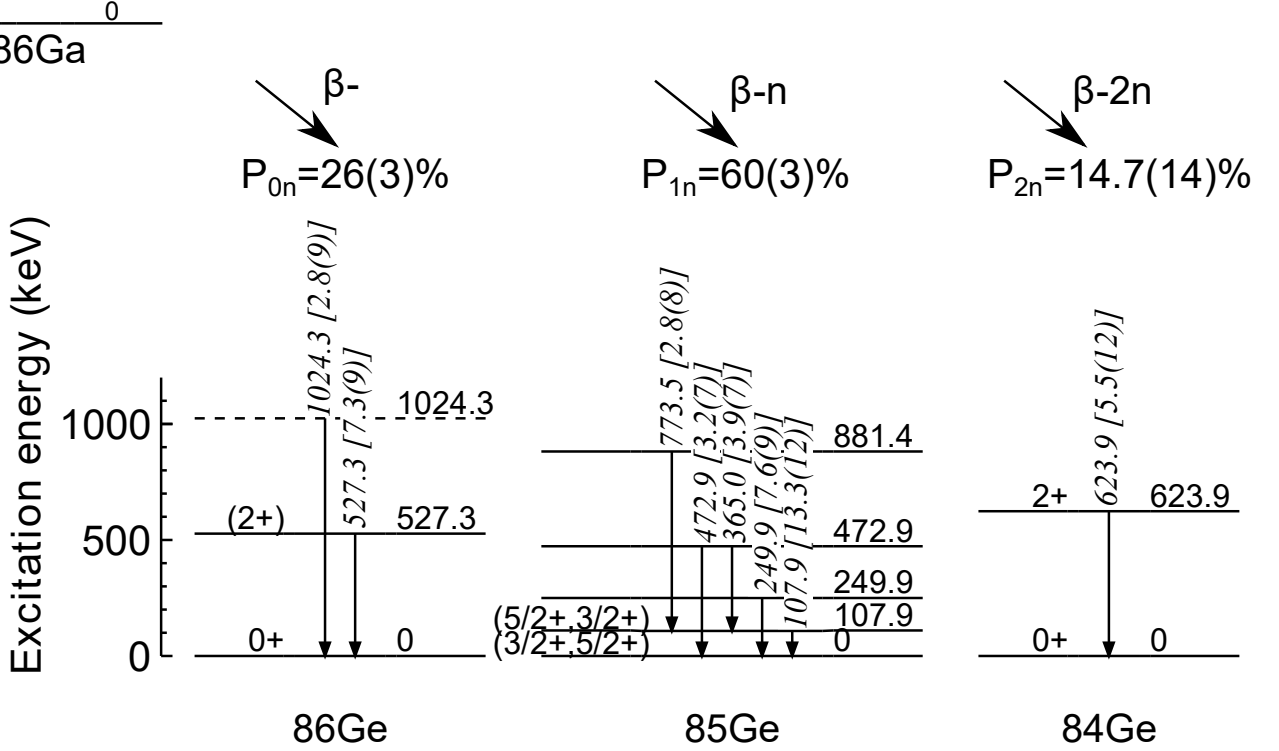


FIG. 10. Level scheme of  $^{84-86}\text{Ge}$  populated in the  $\beta$  decays of  $^{86}\text{Ga}$ . Spin-parity assignments are from Refs. [56, 60, 61]. Intensities of the  $\gamma$  transitions in square parentheses are given per 100  $^{86}\text{Ga}$  decays.

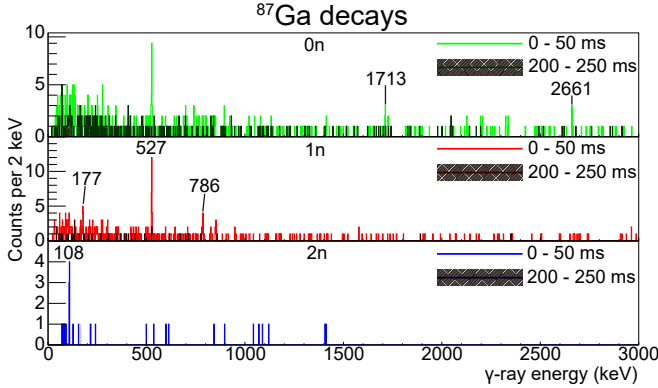


FIG. 11. Gamma-ray energy spectra of  $^{87}\text{Ga}$  gated by neutron multiplicities.

viously described in [34, 69, 70]. In this model, the beta-decay properties are dominated by the Gamow-Teller decay of the  $^{78}\text{Ni}$ -core states, leaving the nucleus in the highly excited state because of the  $N = 50$  shell gap. Good agreement between the  $1n$  emission data predicted by the shell model and experimental data was achieved by choosing the 50% quenching factor for the B(GT), which was deduced from the experimental neutron spectrum and adding the contribution from forbidden transitions.

An essential element of the description of this decay process in this framework is the contribution from the

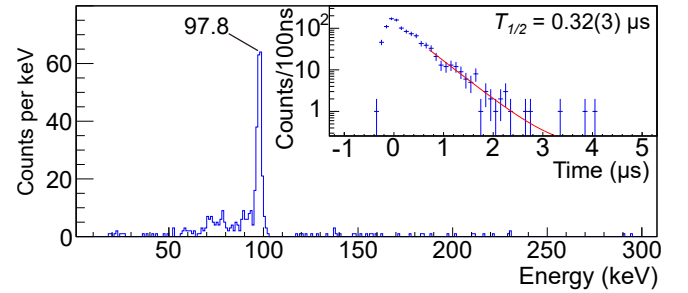


FIG. 12. Delayed  $\gamma$ -ray energy spectrum from 600 ns to 3  $\mu\text{s}$  after implantation of the  $^{86}\text{Ga}$  ion. The plot at the top right corner shows the decay curve of the 97.8 keV  $\gamma$  line.

first forbidden transitions to the low excited states in Ge daughters. Despite their tiny matrix elements, their intensities are amplified by the phase space factor and result in a significant population of the neutron-bound states and, thus, suppresses the branching ratio of neutron emission channels. The inherent uncertainties of the B(GT)+FF models as well as decay energies and neutron separation energies require estimates of the expected lifetimes and  $P_{xn}$ . This was done by varying the scaling factor of the forbidden transition strength and shifting the B(GT) distribution. This analysis is required to find a possible scenario for the decay strength distribution, which will explain experimental data on  $T_{1/2}$  and  $P_{0n}$  at

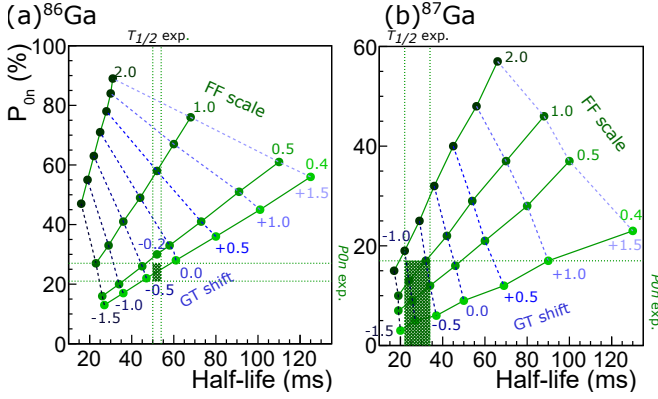


FIG. 13.  $P_{0n}$  versus  $T_{1/2}$  plot for the shell-model calculations on  $^{86,87}\text{Ga}$ . The hatched areas in the plots represent the experimental error bars on those values.

the same time. We assumed B(GT) 50% quenching from Madurga *et al.* in our model and kept it constant. The FF strength was constrained by  $P_{0n}$  and lifetimes. The concentration of the B(GT) to highly excited, neutron-emitting states in Ge isotopes is the main reason why given the large Q values, the nuclear lifetimes for Ga isotopes are relatively long. Figure 13 (a) and (b) shows the  $P_{0n}$  versus  $T_{1/2}$  plots for  $^{86,87}\text{Ga}$  with various offsets of the B(GT) distribution (GT shift) and scaling factors on the FF distribution (FF scale). Unlike  $P_{1n}/P_{2n}$ ,  $P_{0n}$  is much less sensitive to the decay models since it almost only depends on the  $\beta$ -decay intensity below the  $S_{1n}$  level which is mostly the FF component. We selected the GT shift and FF scale, -0.2 and 0.4 for  $^{86}\text{Ga}$ , and -1.0 and 0.5 for  $^{87}\text{Ga}$ .

The GT shift and FF scale values were also used in the calculations shown in the previous paper [31], which demonstrated that the statistical model correctly reproduces the dominating role of one-neutron emission from two-neutron unbound states.

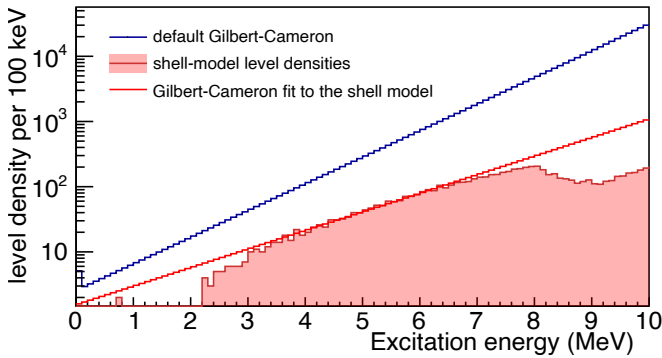


FIG. 14. Comparison of the default Gilbert-Cameron level densities in the statistical model and those from the shell-model calculation for  $^{85}\text{Ge}$ .

As we calculated the branching ratios by the statistical model, we found that the decay patterns were sensitive to the level densities of the daughter nuclei. In the statis-

tical model code by Kawano *et al.*[38], shell and pairing energies from the mass formula by Koura *et al.*, KTUY05, were applied to the Gilbert-Cameron formula [71] to generate phenomenological nuclear level densities [72]. The shell and pairing corrections were applied to the constant temperature level density formula,

$$\rho = \frac{1}{T} \exp\left(\frac{E - E_0}{T}\right) \quad (5)$$

as the energy shift,  $E_0$ , and the systematic temperature,  $T_{syst}$ , which are defined as follows.

$$\begin{aligned} E_0 &= \Delta - \gamma_2 \delta w + T_{syst} f(A) \\ T_{syst} &= \eta_1 A^{-\epsilon_1} \sqrt{1 - \gamma_1 \delta w}. \end{aligned} \quad (6)$$

$\Delta$  and  $\delta w$  are the pairing energy and the shell correction, respectively, from the KTUY05 data. The smooth function of the mass number,  $f(A)$ , is defined in Ref. [72]. Also, a scaling factor,  $f_{tweak}$ , was applied to the temperature:

$$T = T_{syst} / f_{tweak}. \quad (7)$$

The blue curve in Fig. 14 shows the default level density for  $^{85}\text{Ge}$  which is higher than the shell-model level densities shown as the red curve in the figure. To calculate the level densities, the NuShellX code with the jj45pna interaction was used to obtain as many states as possible. Due to our computational limit, levels up to  $\approx 7$  MeV were calculated for all the spins and parities. We fitted the shell-model level densities by Eq. 5 where  $\delta w$ ,  $\Delta$ , and  $f_{tweak}$  were free parameters. The level density function fitted for  $^{85}\text{Ge}$  is shown as a red curve in Fig. 14. The fitting parameters for  $^{83-86}\text{Ge}$  are summarized in Table. VI.

TABLE VI. List of parameters for the level density function.

nuclide	default		fit		
	$\delta w$	$\Delta$	$\delta w$	$\Delta$	$f_{tweak}$
$^{83}\text{Ge}$	-3.71710	1.44894	4.88176	0.00000	0.147891
$^{84}\text{Ge}$	-3.07530	2.29824	-9.06038	4.03678	0.661307
$^{85}\text{Ge}$	-2.52280	1.44090	-7.41890	4.22327	0.786374
$^{86}\text{Ge}$	-1.83290	2.27325	-7.50608	4.20162	0.780135

Statistical model calculations were performed on the decay of Ga isotopes with the default and the shell-model level densities of the daughter nuclei. Figure 15 shows the population of the excited states in the Ge daughters in the decay of  $^{86}\text{Ga}$ . The  $\beta$ -decay feeding intensity in  $^{86}\text{Ge}$  was based on the shell-model calculation. Only the GT part is considered in this plot because the FF part only affects  $P_{0n}$  but not 1n/2n competition. The excited states in  $^{85,84}\text{Ge}$  are from the fitted level density but the low-lying levels are replaced with our experimental level schemes.

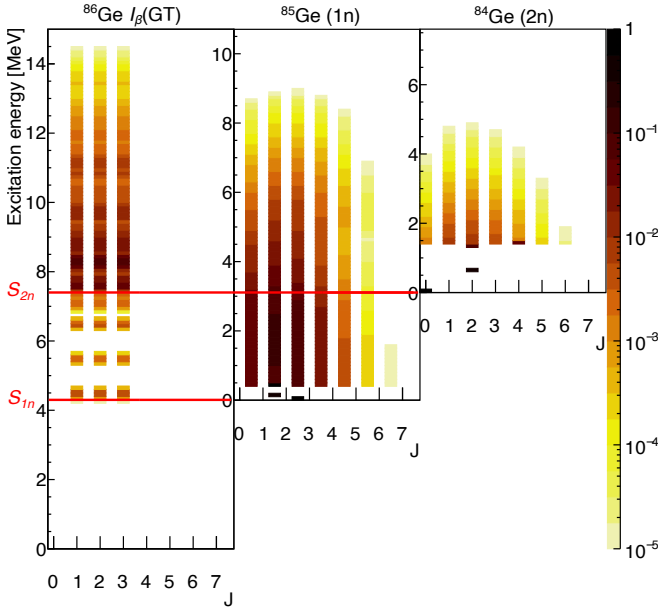


FIG. 15. Populations of the states excited by particle emission after the decay of  $^{86}\text{Ga}$  simulated by the statistical model.  $J^\pi = 2^-$  was assumed for the ground state of  $^{86}\text{Ga}$

As shown in Fig. 16,  $P_{2n}/P_{1n}$  ratios changes by using different level densities in the statistical model calculations. The default level densities, which are higher than the shell-model ones, consistently predicted larger  $P_{2n}$  ratios for all four Ga isotopes. The higher level density above  $S_{1n}$  in the 1n daughter nucleus can result in a higher probability of emitting a second neutron. The experimental ratios agree better with the calculations with the shell-model level densities, which could mean the level densities of those Ge isotopes are lower than what was used in the statistical model with default parameters provided that we operate in compound nucleus approximation.

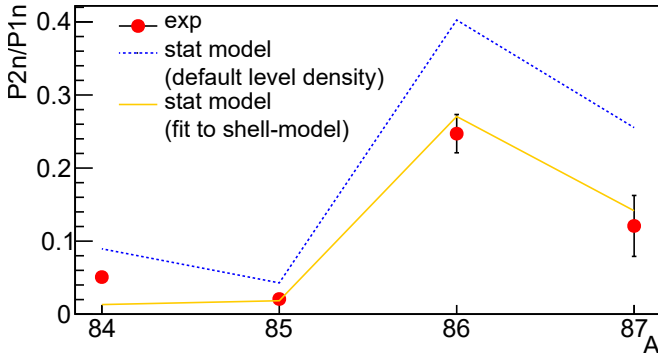


FIG. 16.  $P_{2n}/P_{1n}$  ratio in the decay of Ga isotopes. The red circle shows the experimental value while the blue-dashed and orange-solid lines show the shell model predictions by using default and shell-model based parameters for the Gilbert-Cameron level densities, respectively.

The ground-state spin and parity ( $J^\pi$ ) of the odd-odd

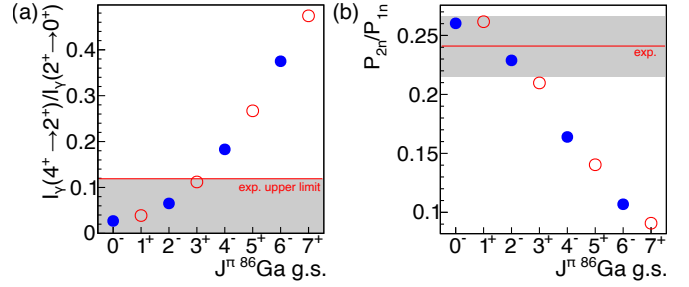


FIG. 17. Comparison of branching ratios calculated by the statistical model with the modified level densities with different assumptions on the unknown  $J^\pi$  of the parent nucleus in the decay of  $^{86}\text{Ga}$ . Only odd spins for positive and even spins for negative parity states are presented for the sake of clarity. The blue circles and red open circles show negative and positive parity states, respectively. (a)  $\gamma$ -ray intensity ratio between  $4^+ \rightarrow 2^+$  (805 keV) and  $2^+ \rightarrow 0^+$  (624 keV) transitions of the  $^{84}\text{Ge}$  nuclei in the 2n decay of  $^{86}\text{Ga}$ . Since the  $4^+$  decay  $\gamma$  line was not observed, the experimental upper limit (see text for detail) is indicated by the red horizontal line. (b)  $P_{2n}/P_{1n}$  ratio. The red line shows the experimental value with a grey error band.

$^{86}\text{Ga}$  nucleus is not known. We compared the  $P_{2n}/P_{1n}$  ratio and  $\gamma$ -ray branching ratio in the decay of  $^{86}\text{Ga}$  by changing the input  $J^\pi$  of the statistical model calculation. As shown in Fig. 17, the statistical model predicts a clear trend of the  $\gamma$ -ray intensity ratio from the  $4^+$  and  $2^+$  states in the 2n decay channel increasing when the initial spin of the parent nucleus is increased. The  $P_{2n}/P_{1n}$  branching ratio, on the other hand, decreases for a higher  $J$ . In this work, the  $4^+ \rightarrow 2^+$   $\gamma$  line was not observed at 805 keV in the 2n gated spectrum (Fig. 9). The background level of the corresponding energy region was estimated to be  $\approx 0.1$  counts/keV by the log-likelihood fitting of the neighboring region around 805 keV. We set the minimum number of counts per keV to 3 as the detection limit of the 805-keV  $\gamma$  peak and deduced the upper limit of the  $I_\gamma(4^+ \rightarrow 2^+)/I_\gamma(2^+ \rightarrow 0^+)$  the ratio of 0.12, which is shown as a gray area in Fig 17 (a). The probability of observing three counts within a one-keV width bin by statistical fluctuation when the background rate is  $0.1$  is  $1.5 \times 10^{-4}$ , which is between  $3\sigma$  and  $4\sigma$ . In Fig. 17 (b), the experimental  $P_{2n}/P_{1n}$  value is shown with an error of  $1\sigma$ . In both plots, the lower spin scenarios ( $J \leq 3$ ) agree with our experimental values.

These results show the importance of the knowledge of the level densities and the ground-state spin of the parent nuclei for making reliable predictions of the multi-neutron emissions, and the requirement of further studies of neutron and  $\gamma$ -ray spectrum to establish details of the emission process.

## V. CONCLUSIONS

In summary, we performed  $\beta$ - $\gamma$ -neutron analysis on  $^{84-87}\text{Ga}$  isotopes and performed statistical model calculations by using the experimental and shell-model levels in the daughter nuclei instead of the default level densities used in the code. We found that the multi-neutron emission ratio ( $P_{2n}/P_{1n}$ ) is sensitive to the level density of the  $A - 1$  daughter nucleus,  $^{83-86}\text{Ge}$ , in this case. The statistical model calculation best reproduced the experimental  $P_{2n}/P_{1n}$  ratio when experimental levels + shell-model level densities fitted by the Gilbert-Cameron formula are used as input. The neutron efficiencies of the BRIKEN array for each isotope were estimated by assuming the neutron spectra from the statistical model calculation to narrow down the systematic uncertainties in  $P_{xn}$  measurements. The  $P_{xn}$  values are updated from the ones reported in the previous paper [31] with a better estimation of neutron efficiencies. For  $^{86}\text{Ga}$  decay, analysis of the neutron and  $\gamma$  branching ratio with the updated statistical model calculation suggests low spin for the ground state of the parent nucleus. These results show the importance of using correct level densities for the  $P_{xn}$  calculation and the necessity of neutron spectroscopy in addition to  $\gamma$  measurements of the multi-neutron emitters.

## ACKNOWLEDGMENTS

This experiment was performed at the RI Beam Factory operated by RIKEN Nishina Center and CNS, University of Tokyo. This research was sponsored in part by the Office of Nuclear Physics, U.S. Department of Energy under Award No. DE-FG02-96ER40983 (UTK) and DE-AC05-00OR22725 (ORNL), No. DE-SC0016988 (TTU) and by the National Nuclear Security Administration under the Stewardship Science Academic Alliances program through DOE Award No. DE-NA0002132. This work was supported by National Science Foun-

ation under Grants No. PHY-1430152 (JINA Center for the Evolution of the Elements), No. PHY-1565546 (NSCL), and No. PHY-1714153 (Central Michigan University). This work was partially funded by the Polish National Science Center under Contracts No. UMO-2015/18/E/ST2/00217, 2020/39/B/ST2/02346, and No. 2017/01/X/ST2/01144. This work was also supported by JSPS KAKENHI (Grants No. 14F04808, No. 17H06090, No. 25247045, 20H05648, 22H04946 and No. 19340074), by the UK Science and Technology Facilities Council, by NKFIH (NN128072), by Spanish Ministerio de Economía y Competitividad grants (FPA2011-06419, FPA2011-28770-C03-03, FPA2014-52823-C2-1-P, FPA2014-52823-C2-2-P, SEV-2014-0398, IJCI-2014-19172), by Generalitat Valenciana regional grant PROMETEO/2019/007, by European Commission FP7/EURATOM Contract No. 605203, by the UK Science and Technology Facilities Council Grant No. ST/N00244X/1, ST//P004598/1, and ST/V001027/1 by the National Research Foundation (NRF) in South Korea (No. 2016K1A3A7A09005575, No. 2015H1A2A1030275) and by the Natural Sciences and Engineering Research Council of Canada (NSERC) via the Discovery Grants SAPIN-2014-00028 and RGPAS 462257-2014. TRIUMF receives federal funding via a contribution agreement with the National Research Council of Canada. The author, R.Y. acknowledges support from JSPS KAKENHI 22K14053. G.G.K. acknowledges support from the Janos Bolyai research fellowship of the Hungarian Academy of Sciences. M.W.-C. acknowledges support from the Polish NCN project Miniatura No. 2017/01/X/ST2/01144. M.P.-S. acknowledges support from Polish National Science Center No. 2019/33/N/ST2/03023 and 2020/36/T/ST2/00547. T.K. carried out this work under the auspices of the National Nuclear Security Administration of the U.S. Department of Energy at Los Alamos National Laboratory under Contract No. 89233218CNA000001. A. A. Acknowledges partial support of the JSPS Invitational Fellowships for Research in Japan (ID: L1955). All of the relevant data of this study are available from the corresponding author upon reasonable request.

- 
- [1] R. B. Roberts, R. C. Meyer, and P. Wang, *Physical Review* **55**, 510 (1939).
- [2] J. Liang, B. Singh, E. A. McCutchan, I. Dillmann, M. Birch, A. A. Sonzogni, X. Huang, M. Kang, J. Wang, G. Mukherjee, K. Banerjee, D. Abriola, A. Algora, A. A. Chen, T. D. Johnson, and K. Miernik, *Nuclear Data Sheets* **168**, 1 (2020).
- [3] P. Dimitriou, I. Dillmann, B. Singh, V. Piksaikin, K. Rykaczewski, J. Tain, A. Algora, K. Banerjee, I. Borzov, D. Cano-Ott, S. Chiba, M. Fallot, D. Foligno, R. Grzywacz, X. Huang, T. Marketin, F. Minato, G. Mukherjee, B. Rasco, A. Sonzogni, M. Verpelli, A. Egorov, M. Estienne, L. Giot, D. Gremyachkin, M. Madurga, E. McCutchan, E. Mendoza, K. Mitrofanov, M. Narbonne, P. Romojaro, A. Sanchez-Caballero, and N. Scielzo, *Nuclear Data Sheets* **173**, 144 (2021), special Issue on Nuclear Reaction Data.
- [4] R. Surman, M. Mumpower, and A. Aprahamian, in *JPS Conference Proceedings*, Vol. 6 (Tokyo, Japan, 2015) p. 010010.
- [5] P. Möller, B. Pfeiffer, and K.-L. Kratz, *Physical Review C* **67**, 055802 (2003).
- [6] T. Marketin, L. Huther, and G. Martínez-Pinedo, *Phys. Rev. C* **93**, 025805 (2016).
- [7] F. Minato, T. Marketin, and N. Paar, *Phys. Rev. C* **104**, 044321 (2021).
- [8] A. Korgul, K. P. Rykaczewski, J. A. Winger, S. V. Ilyushkin, C. J. Gross, J. C. Batchelder, C. R. Bing-

- ham, I. N. Borzov, C. Goodin, R. Grzywacz, J. H. Hamilton, W. Królas, S. N. Liddick, C. Mazzocchi, C. Nelson, F. Nowacki, S. Padgett, A. Piechaczek, M. M. Rajabali, D. Shapira, K. Sieja, and E. F. Zganjar, *Phys. Rev. C* **86**, 024307 (2012).
- [9] J. L. Tain, E. Valencia, A. Algora, J. Agramunt, B. Rubio, S. Rice, W. Gelletly, P. Regan, A. A. Zakari-Issoufou, M. Fallot, A. Porta, J. Rissanen, T. Eronen, J. Äystö, L. Batist, M. Bowry, V. M. Bui, R. Caballero-Folch, D. Cano-Ott, V. V. Elomaa, E. Estevez, G. F. Farrelly, A. R. Garcia, B. Gomez-Hornillos, V. Gorlychev, J. Hakala, M. D. Jordan, A. Jokinen, V. S. Kolhinen, F. G. Kondev, T. Martínez, E. Mendoza, I. Moore, H. Penttilä, Z. Podolyák, M. Reponen, V. Sonnenschein, and A. A. Sonzogni, *Physical Review Letters* **115**, 062502 (2015).
- [10] B. C. Rasco, K. P. Rykaczewski, A. Fijałkowska, M. Karny, M. Wolińska-Cichocka, R. K. Grzywacz, C. J. Gross, D. W. Stracener, E. F. Zganjar, J. C. Blackmon, N. T. Brewer, K. C. Goetz, J. W. Johnson, C. U. Jost, J. H. Hamilton, K. Miernik, M. Madurga, D. Miller, S. Padgett, S. V. Paulauskas, A. V. Ramayya, and E. H. Spejewski, *Physical Review C* **95**, 054328 (2017).
- [11] A. Spyrou, S. N. Liddick, F. Naqvi, B. P. Crider, A. C. Dombos, D. L. Bleuel, B. A. Brown, A. Couture, L. Crespo Campo, M. Guttormsen, A. C. Larsen, R. Lewis, P. Möller, S. Mosby, M. R. Mumpower, G. Perdikakis, C. J. Prokop, T. Renstrøm, S. Siem, S. J. Quinn, and S. Valenta, *Physical Review Letters* **117**, 142701 (2016).
- [12] T. Kawano, P. Talou, I. Stetcu, and M. B. Chadwick, *Nuclear Physics A* **913**, 51 (2013).
- [13] M. R. Mumpower, T. Kawano, and P. Möller, *Physical Review C* **94**, 064317 (2016).
- [14] P. Möller, M. R. Mumpower, T. Kawano, and W. D. Myers, *Atomic Data and Nuclear Data Tables* **125**, 1 (2019), arXiv:9601043 [nucl-th].
- [15] R. E. Azuma, L. C. Carraz, P. G. Hansen, B. Jonson, K. L. Kratz, S. Mattsson, G. Nyman, H. Ohm, H. L. Ravn, A. Schroder, and W. Ziegert, *Physical Review Letters* **43**, 1652 (1979).
- [16] J. Dufour, R. Delmoral, F. Hubert, D. Jean, M. Pravikoff, A. Fleury, A. Mueller, K.-H. Schmidt, K. Summerer, E. Hanelt, J. Frehaut, M. Meau, and G. Giraudet, *Physics Letters B* **206**, 195 (1988).
- [17] K. Yoneda, N. Aoi, H. Iwasaki, H. Sakurai, H. Ogawa, T. Nakamura, W.-D. Schmidt-Ott, M. Schäfer, M. Notani, N. Fukuda, E. Ideguchi, T. Kishida, S. S. Yamamoto, and M. Ishihara, *Physical Review C* **67**, 014316 (2003).
- [18] V. Tripathi, S. L. Tabor, C. R. Hoffman, M. Wiedeking, A. Volya, P. F. Mantica, A. D. Davies, S. N. Liddick, W. F. Mueller, A. Stolz, B. E. Tomlin, T. Otsuka, and Y. Utsuno, *Physical Review C - Nuclear Physics* **73**, 054303 (2006).
- [19] M. Langevin, C. Détraz, D. Guillemaud-Mueller, A. C. Mueller, C. Thibault, F. Touchard, and M. Epherre, *Nuclear Physics A* **414**, 151 (1984).
- [20] F. Perrot, F. Maréchal, C. Jollet, P. Dessagne, J. C. Angélique, G. Ban, P. Baumann, F. Benrachi, U. Bergmann, C. Borcea, A. Buta, J. Cederkall, S. Courtin, J. M. Daugas, L. M. Fraile, S. Grévy, A. Jokinen, F. R. Lecolley, E. Liénard, G. LeScornet, V. Méot, C. Miehé, F. Negoita, N. A. Orr, S. Pietri, E. Poirier, M. Ramdhane, O. Roig, I. Stefan, and W. Wang, *Physical Review C - Nuclear Physics* **74**, 014313 (2006).
- [21] P. L. Reeder, R. A. Warner, T. R. Yeh, R. E. Chrien, R. L. Gill, M. Shmid, H. I. Liou, and M. L. Stelts, *Physical Review Letters* **47**, 483 (1981).
- [22] B. Jonson, H. Gustafsson, P. Hansen, P. Hoff, P. Larsson, S. Mattsson, G. Nyman, H. Ravn, and D. Schardt, in *Proceedings of the 4th International Conference on Nuclei Far From Stability*, Vol. CERN-81-09 (1981) p. 265.
- [23] R. Caballero-Folch, I. Dillmann, J. Agramunt, J. L. Tain, A. Algora, J. Äystö, F. Calviño, L. Canete, G. Cortès, C. Domingo-Pardo, T. Eronen, E. Ganioğlu, W. Gelletly, D. Gorelov, V. Guadilla, J. Hakala, A. Jokinen, A. Kankainen, V. Kolhinen, J. Koponen, M. Marta, E. Mendoza, A. Montaner-Pizá, I. Moore, C. R. Nobs, S. E. A. Orrigo, H. Penttilä, I. Pohjalainen, J. Reinikainen, A. Riego, S. Rinta-Antila, B. Rubio, P. Salvador-Castiñeira, V. Simutkin, A. Tarifeño Saldivia, A. Tolosa-Delgado, and A. Voss, *Phys. Rev. C* **98**, 034310 (2018).
- [24] K. Miernik, K. P. Rykaczewski, C. J. Gross, R. Grzywacz, M. Madurga, D. Miller, J. C. Batchelder, I. N. Borzov, N. T. Brewer, C. Jost, A. Korgul, C. Mazzocchi, A. J. Mendez, Y. Liu, S. V. Paulauskas, D. W. Stracener, J. A. Winger, M. Wolińska-Cichocka, and E. F. Zganjar, *Physical Review Letters* **111**, 132502 (2013).
- [25] B. Moon, C.-B. Moon, P.-A. Söderström, A. Odahara, R. Lozeva, B. Hong, F. Browne, H. S. Jung, P. Lee, C. S. Lee, A. Yagi, C. Yuan, S. Nishimura, P. Doornenbal, G. Lorusso, T. Sumikama, H. Watanabe, I. Kojouharov, T. Isobe, H. Baba, H. Sakurai, R. Daido, Y. Fang, H. Nishibata, Z. Patel, S. Rice, L. Sinclair, J. Wu, Z. Y. Xu, R. Yokoyama, T. Kubo, N. Inabe, H. Suzuki, N. Fukuda, D. Kameda, H. Takeda, D. S. Ahn, Y. Shimizu, D. Murai, F. L. Bello Garrote, J. M. Daugas, F. Didierjean, E. Ideguchi, T. Ishigaki, S. Morimoto, M. Niikura, I. Nishizuka, T. Komatsubara, Y. K. Kwon, and K. Tshoo, *Physical Review C* **95**, 044322 (2017).
- [26] M. Piersa-Siłkowska, A. Korgul, J. Benito, L. M. Fraile, E. Adamska, A. N. Andreyev, R. Álvarez-Rodríguez, A. E. Barzakh, G. Benzoni, T. Berry, M. J. G. Borge, M. Carmona, K. Chrysalidis, J. G. Correia, C. Costache, J. G. Cubiss, T. Day Goodacre, H. De Witte, D. V. Fedorov, V. N. Fedosseev, G. Fernández-Martínez, A. Fijałkowska, H. Fynbo, D. Galaviz, P. Galve, M. García-Díez, P. T. Greenlees, R. Grzywacz, L. J. Harkness-Brennan, C. Henrich, M. Huyse, P. Ibáñez, A. Ilana, Z. Janas, K. Johnston, J. Jolie, D. S. Judson, V. Karanyonchev, M. Kicińska Habior, J. Konki, L. Koszuck, J. Kurcewicz, I. Lazarus, R. Lică, A. López-Montes, H. Mach, M. Madurga, I. Marroquín, B. Marsh, M. C. Martínez, C. Mazzocchi, K. Miernik, C. Mihai, N. Mărginean, R. Mărginean, A. Negret, E. Năcher, J. Ojala, B. Olaizola, R. D. Page, J. Pakarinen, S. Pascu, S. V. Paulauskas, A. Perea, V. Pucknell, P. Rauhila, C. Raison, E. Rapisarda, K. Rezyńska, F. Rotaru, S. Rothe, K. P. Rykaczewski, J.-M. Régis, K. Schomacker, M. Siłkowski, G. Simpson, C. Sotty, L. Stan, M. Stănoiu, M. Stryczyk, D. Sánchez-Parcerisa, V. Sánchez-Tembleque, O. Tengblad, A. Turturică, J. M. Udias, P. Van Duppen, V. Vedia, A. Villa, S. Viñals, R. Wadsworth, W. B. Walters, N. Warr, and S. G. Wilkins (IDS Collaboration), *Phys. Rev. C* **104**, 044328 (2021).

- [27] J. Pereira, P. Hosmer, G. Lorusso, P. Santi, A. Couture, J. Daly, M. D. Santo, T. Elliot, J. Görres, C. Herlitzius, K. L. Kratz, L. O. Lamm, H. Y. Lee, F. Montes, M. Ouellette, E. Pellegrini, P. Reeder, H. Schatz, F. Schertz, L. Schnorrenberger, K. Smith, E. Stech, E. Strandberg, C. Ugalde, M. Wiescher, and A. Wöhr, *Nuclear Instruments and Methods in Physics Research, Section A: Accelerators, Spectrometers, Detectors and Associated Equipment* **618**, 275 (2010).
- [28] R. Grzywacz, K. P. Rykaczewski, C. J. Gross, M. Madurga, K. Miernik, D. T. Miller, S. V. Paulauskas, S. W. Padgett, C. Rasco, M. Wolińska-Cichocka, and E. F. Zganjar, *Acta Physica Polonica B* **45**, 217 (2014).
- [29] M. B. Gómez-Hornillos, J. Rissanen, J. L. Taín, A. Algora, D. Cano-Ott, J. Agramunt, V. Gorlychev, R. Caballero, T. Martínez, L. Achouri, J. Äystö, G. Cortés, V. V. Elomaa, T. Eronen, A. García, J. Hakala, A. Jokinen, P. Karvonen, V. S. Kolhinen, I. Moore, M. Parlog, H. Penttilä, Z. Podolyak, C. Pretel, M. Reponen, V. Sonnenschein, and E. Valencia, *Journal of Physics: Conference Series* **312**, 052008 (2011).
- [30] A. Tarifeño-Saldivia, J. L. Tain, C. Domingo-Pardo, F. Calviño, G. Cortés, V. H. Phong, A. Riego, J. Agramunt, A. Algora, N. Brewer, R. Caballero-Folch, P. J. Coleman-Smith, T. Davinson, I. Dillmann, A. Estradé, C. J. Griffin, R. Grzywacz, L. J. Harkness-Brennan, G. G. Kiss, M. Kogimtzis, M. Labiche, I. H. Lazarus, G. Lorusso, K. Matsui, K. Miernik, F. Montes, A. I. Morales, S. Nishimura, R. D. Page, Z. S. Podolyák, V. F. Pucknell, B. C. Rasco, P. Regan, B. Rubio, K. P. Rykaczewski, Y. Saito, H. Sakurai, J. Simpson, E. Sokol, R. Surman, A. Svirikhin, S. L. Thomas, A. Tolosa, and P. Woods, *Journal of Instrumentation* **12**, P04006 (2017).
- [31] R. Yokoyama, R. Grzywacz, B. C. Rasco, N. Brewer, K. P. Rykaczewski, I. Dillmann, J. L. Tain, S. Nishimura, D. S. Ahn, A. Algora, J. M. Allmond, J. Agramunt, H. Baba, S. Bae, C. G. Bruno, R. Caballero-Folch, F. Calviño, P. J. Coleman-Smith, G. Cortes, T. Davinson, C. Domingo-Pardo, A. Estrade, N. Fukuda, S. Go, C. J. Griffin, J. Ha, O. Hall, L. J. Harkness-Brennan, J. Heideman, T. Isobe, D. Kahl, M. Karny, T. Kawano, L. H. Khiem, T. T. King, G. G. Kiss, A. Korgul, S. Kubono, M. Labiche, I. Lazarus, J. Liang, J. Liu, G. Lorusso, M. Madurga, K. Matsui, K. Miernik, F. Montes, A. I. Morales, P. Morrall, N. Nepal, R. D. Page, V. H. Phong, M. Piersa, M. Prydderch, V. F. E. Pucknell, M. M. Rajabali, B. Rubio, Y. Saito, H. Sakurai, Y. Shimizu, J. Simpson, M. Singh, D. W. Stracener, T. Sumikama, R. Surman, H. Suzuki, H. Takeda, A. Tarifeño Saldivia, S. L. Thomas, A. Tolosa-Delgado, M. Wolińska Cichocka, P. J. Woods, and X. X. Xu, *Phys. Rev. C* **100**, 031302 (2019).
- [32] O. Hall, T. Davinson, A. Estrade, J. Liu, G. Lorusso, F. Montes, S. Nishimura, V. Phong, P. Woods, J. Agramunt, D. Ahn, A. Algora, J. Allmond, H. Baba, S. Bae, N. Brewer, C. Bruno, R. Caballero-Folch, F. Calviño, P. Coleman-Smith, G. Cortes, I. Dillmann, C. Domingo-Pardo, A. Fijalkowska, N. Fukuda, S. Go, C. Griffin, R. Grzywacz, J. Ha, L. Harkness-Brennan, T. Isobe, D. Kahl, L. Khiem, G. Kiss, A. Korgul, S. Kubono, M. Labiche, I. Lazarus, J. Liang, Z. Liu, K. Matsui, K. Miernik, B. Moon, A. Morales, P. Morrall, M. Mumpower, N. Nepal, R. Page, M. Piersa, V. Pucknell, B. Rasco, B. Rubio, K. Rykaczewski, H. Sakurai, Y. Shimizu, D. Stracener, T. Sumikama, H. Suzuki, J. Tain, H. Takeda, A. Tarifeño-Saldivia, A. Tolosa-Delgado, M. Wolińska-Cichocka, and R. Yokoyama, *Physics Letters B* **816**, 136266 (2021).
- [33] V. H. Phong, S. Nishimura, G. Lorusso, T. Davinson, A. Estrade, O. Hall, T. Kawano, J. Liu, F. Montes, N. Nishimura, R. Grzywacz, K. P. Rykaczewski, J. Agramunt, D. S. Ahn, A. Algora, J. M. Allmond, H. Baba, S. Bae, N. T. Brewer, C. G. Bruno, R. Caballero-Folch, F. Calviño, P. J. Coleman-Smith, G. Cortes, I. Dillmann, C. Domingo-Pardo, A. Fijalkowska, N. Fukuda, S. Go, C. J. Griffin, J. Ha, L. J. Harkness-Brennan, T. Isobe, D. Kahl, L. H. Khiem, G. G. Kiss, A. Korgul, S. Kubono, M. Labiche, I. Lazarus, J. Liang, Z. Liu, K. Matsui, K. Miernik, B. Moon, A. I. Morales, P. Morrall, N. Nepal, R. D. Page, M. Piersa-Siłkowska, V. F. E. Pucknell, B. C. Rasco, B. Rubio, H. Sakurai, Y. Shimizu, D. W. Stracener, T. Sumikama, H. Suzuki, J. L. Tain, H. Takeda, A. Tarifeño Saldivia, A. Tolosa-Delgado, M. Wolińska Cichocka, P. J. Woods, and R. Yokoyama, *Phys. Rev. Lett.* **129**, 172701 (2022).
- [34] M. Madurga, S. V. Paulauskas, R. Grzywacz, D. Miller, D. W. Bardayan, J. C. Batchelder, N. T. Brewer, J. A. Cizewski, A. Fijalkowska, C. J. Gross, M. E. Howard, S. V. Ilyushkin, B. Manning, M. Matoš, A. J. Mendez, K. Miernik, S. W. Padgett, W. A. Peters, B. C. Rasco, A. Ratkiewicz, K. P. Rykaczewski, D. W. Stracener, E. H. Wang, M. Wolińska-Cichocka, and E. F. Zganjar, *Physical Review Letters* **117**, 092502 (2016).
- [35] J. A. Winger, S. V. Ilyushkin, K. P. Rykaczewski, C. J. Gross, J. C. Batchelder, C. Goodin, R. Grzywacz, J. H. Hamilton, A. Korgul, W. Królas, S. N. Liddick, C. Mazzocchi, S. Padgett, A. Piechaczek, M. M. Rajabali, D. Shapira, E. F. Zganjar, and I. N. Borzov, *Physical Review Letters* **102**, 142502 (2009).
- [36] K. Miernik, K. P. Rykaczewski, R. Grzywacz, C. J. Gross, M. Madurga, D. Miller, D. W. Stracener, J. C. Batchelder, N. T. Brewer, A. Korgul, C. Mazzocchi, A. J. Mendez, Y. Liu, S. V. Paulauskas, J. A. Winger, M. Wolińska Cichocka, and E. F. Zganjar, *Phys. Rev. C* **97**, 054317 (2018).
- [37] D. Verney, D. Testov, F. Ibrahim, Y. Penionzhkevich, B. Roussière, V. Smirnov, F. Didierjean, K. Flanagan, S. Franchoo, E. Kuznetsova, R. Li, B. Marsh, I. Matea, H. Pai, E. Sokol, I. Stefan, and D. Suzuki, *Physical Review C* **95**, 054320 (2017).
- [38] T. Kawano, P. Möller, and W. B. Wilson, *Physical Review C - Nuclear Physics* **78**, 054601 (2008).
- [39] T. Kubo, *Nuclear Instruments and Methods in Physics Research Section B: Beam Interactions with Materials and Atoms* **204**, 97 (2003).
- [40] H. Kumagai, A. Ozawa, N. Fukuda, K. Sümmerer, and I. Tanihata, *Nuclear Instruments and Methods in Physics Research Section A: Accelerators, Spectrometers, Detectors and Associated Equipment* **470**, 562 (2001).
- [41] K. Kimura, T. Izumikawa, R. Koyama, T. Ohnishi, T. Ohtsubo, a. Ozawa, W. Shinozaki, T. Suzuki, M. Takahashi, I. Tanihata, T. Yamaguchi, and Y. Yamaguchi, *Nuclear Instruments and Methods in Physics Research, Section A: Accelerators, Spectrometers, Detectors and Associated Equipment* **538**, 608 (2005).
- [42] T. Ohnishi, T. Kubo, K. Kusaka, A. Yoshida, K. Yoshida, M. Ohtake, N. Fukuda, H. Takeda, D. Kameda, K. Tanaka, N. Inabe, Y. Yanagisawa, Y. Gono, H. Watan-

- abe, H. Otsu, H. Baba, T. Ichihara, Y. Yamaguchi, M. Takechi, S. Nishimura, H. Ueno, A. Yoshimi, H. Sakurai, T. Motobayashi, T. Nakao, Y. Mizoi, M. Matsushita, K. Ieki, N. Kobayashi, K. Tanaka, Y. Kawada, N. Tanaka, S. Deguchi, Y. Satou, Y. Kondo, T. Nakamura, K. Yoshinaga, C. Ishii, H. Yoshii, Y. Miyashita, N. Uematsu, Y. Shiraki, T. Sumikama, J. Chiba, E. Ideguchi, A. Saito, T. Yamaguchi, I. Hachiuma, T. Suzuki, T. Moriguchi, A. Ozawa, T. Ohtsubo, M. a. Famiano, H. Geissel, A. S. Nettleton, O. B. Tarasov, D. P. Bazin, B. M. Sherrill, S. L. Manikonda, and J. a. Nolen, *Journal of the Physical Society of Japan* **79**, 073201 (2010).
- [43] N. Fukuda, T. Kubo, T. Ohnishi, N. Inabe, H. Takeda, D. Kameda, and H. Suzuki, *Nuclear Instruments and Methods in Physics Research Section B: Beam Interactions with Materials and Atoms* **317**, 323 (2013).
- [44] O. Hall, T. Davinson, C. Griffin, P. Woods, C. Appleton, C. Bruno, A. Estrade, D. Kahl, L. Sexton, I. Burrows, P. Coleman-Smith, M. Cordwell, A. Grant, M. Kogimtzis, M. Labiche, J. Lawson, I. Lazarus, P. Morall, V. Pucknell, J. Simpson, C. Unsworth, D. Braga, M. Prydderch, S. Thomas, L. Harkness-Brennan, P. Nolan, R. Page, and D. Seddon, *Nuclear Instruments and Methods in Physics Research Section A: Accelerators, Spectrometers, Detectors and Associated Equipment* **1050**, 168166 (2023).
- [45] S. Nishimura, G. Lorusso, Z. Xu, J. Wu, R. Gernh, H. S. Jung, Y. K. Kwon, Z. Li, K. Steiger, and H. Sakurai, *RIKEN Accelerator Progress Report* **46**, 182 (2013).
- [46] R. Yokoyama, M. Singh, R. Grzywacz, A. Keeler, T. T. King, J. Agramunt, N. T. Brewer, S. Go, J. Heide-man, J. Liu, S. Nishimura, P. Parkhurst, V. H. Phong, M. M. Rajabali, B. C. Rasco, K. P. Rykaczewski, D. W. Stracener, J. L. Tain, A. Tolosa-Delgado, K. Vaigneur, and M. Wolińska-Cichocka, *Nuclear Instruments and Methods in Physics Research, Section A: Accelerators, Spectrometers, Detectors and Associated Equipment* **937**, 93 (2019).
- [47] E. Sahin, F. L. Bello Garrote, Y. Tsunoda, T. Otsuka, G. de Angelis, A. Görgen, M. Niikura, S. Nishimura, Z. Y. Xu, H. Baba, F. Browne, M.-C. Delattre, P. Doornenbal, S. Franchoo, G. Gey, K. Hadyńska-Klęk, T. Isobe, P. R. John, H. S. Jung, I. Kojouharov, T. Kubo, N. Kurz, Z. Li, G. Lorusso, I. Matea, K. Matsui, D. Mengoni, P. Morfouace, D. R. Napoli, F. Naqvi, H. Nishibata, A. Odahara, H. Sakurai, H. Schaffner, P.-A. Söderström, D. Sohler, I. G. Stefan, T. Sumikama, D. Suzuki, R. Taniuchi, J. Taprogge, Z. Vajta, H. Watanabe, V. Werner, J. Wu, A. Yagi, M. Yalcinkaya, and K. Yoshinaga, *Phys. Rev. Lett.* **118**, 242502 (2017).
- [48] A. Tolosa-Delgado, J. Agramunt, J. L. Tain, A. Algora, C. Domingo-Pardo, A. I. Morales, B. Rubio, A. Tarifeño-Saldivia, F. Calviño, G. Cortes, N. T. Brewer, B. C. Rasco, K. P. Rykaczewski, D. W. Stracener, J. M. Allmond, R. Grzywacz, R. Yokoyama, M. Singh, T. King, M. Madurga, S. Nishimura, V. H. Phong, S. Go, J. Liu, K. Matsui, H. Sakurai, G. G. Kiss, T. Isobe, H. Baba, S. Kubono, N. Fukuda, D. S. Ahn, Y. Shimizu, T. Sumikama, H. Suzuki, H. Takeda, P. A. Söderström, M. Takechi, C. Bruno, T. Davinson, C. J. Griffin, O. Hall, D. Kahl, P. J. Woods, P. J. Coleman-Smith, M. Labiche, I. Lazarus, P. Morrall, V. F. E. Pucknell, J. Simpson, S. L. Thomas, M. Prydderch, L. J. Harkness-Brennan, R. D. Page, I. Dillmann, R. Caballero-Folch, Y. Saito, A. Estrade, N. Nepal, F. Montes, G. Lorusso, J. Liang, S. Bae, J. Ha, and B. Moon, *Nuclear Instruments and Methods in Physics Research Section A: Accelerators, Spectrometers, Detectors and Associated Equipment* **925**, 133 (2019).
- [49] B. C. Rasco, N. T. Brewer, R. Yokoyama, R. Grzywacz, K. P. Rykaczewski, A. Tolosa-Delgado, J. Agramunt, J. L. Tain, A. Algora, O. Hall, C. Griffin, T. Davinson, V. H. Phong, J. Liu, S. Nishimura, G. G. Kiss, N. Nepal, and A. Estrade, *Nuclear Instruments and Methods in Physics Research Section A: Accelerators, Spectrometers, Detectors and Associated Equipment* **911**, 79 (2018).
- [50] C. J. Gross, T. N. Ginter, D. Shapira, W. T. Milner, J. W. McConnell, A. N. James, J. W. Johnson, J. Mas, P. F. Mantica, R. L. Auble, J. J. Das, J. L. Blankenship, J. H. Hamilton, R. L. Robinson, Y. A. Akovali, C. Bak-tash, J. C. Batchelder, C. R. Bingham, M. J. Brinkman, H. K. Carter, R. A. Cunningham, T. Davinson, J. D. Fox, A. Galindo-Uribarri, R. Grzywacz, J. F. Liang, B. D. MacDonald, J. MacKenzie, S. D. Paul, A. Piechaczek, D. C. Radford, A. V. Ramayya, W. Reviol, D. Rudolph, K. Rykaczewski, K. S. Toth, W. Weintraub, C. Williams, P. J. Woods, C. H. Yu, and E. F. Zganjar, *Nuclear Instruments and Methods in Physics Research, Section A: Accelerators, Spectrometers, Detectors and Associated Equipment* **450**, 12 (2000).
- [51] C. Mazzocchi, K. P. Rykaczewski, A. Korgul, R. Grzywacz, P. Baczyk, C. Bingham, N. T. Brewer, C. J. Gross, C. Jost, M. Karny, M. Madurga, A. J. Mendez, K. Miernik, D. Miller, S. Padgett, S. V. Paulauskas, D. W. Stracener, M. Wolińska-Cichocka, and I. N. Borzov, *Phys. Rev. C* **87**, 034315 (2013).
- [52] A. Tolosa-Delgado, Ph.D. thesis, University of Valencia (2020).
- [53] K. Kolos, D. Verney, F. Ibrahim, F. Le Blanc, S. Franchoo, K. Sieja, F. Nowacki, C. Bonnin, M. Cheikh Mhamed, P. V. Cuong, F. Didierjean, G. Duchêne, S. Es-sabaa, G. Germogli, L. H. Khiem, C. Lau, I. Matea, M. Niikura, B. Roussi re, I. Stefan, D. Testov, and J. C. Thomas, *Physical Review C - Nuclear Physics* **88**, 047301 (2013).
- [54] J. A. Winger, K. P. Rykaczewski, C. J. Gross, R. Grzywacz, J. C. Batchelder, C. Goodin, J. H. Hamilton, S. V. Ilyushkin, A. Korgul, W. Kr las, S. N. Liddick, C. Mazzocchi, S. Padgett, A. Piechaczek, M. M. Rajabali, D. Shapira, E. F. Zganjar, and J. Dobaczewski, *Physical Review C - Nuclear Physics* **81**, 044303 (2010).
- [55] I. Collaboration, *Zeitschrift f r Physik A* **420**, 419 (1991).
- [56] M. Lettmann, V. Werner, N. Pietralla, P. Doornenbal, A. Obertelli, T. R. Rodr guez, K. Sieja, G. Authelet, H. Baba, D. Calvet, F. Ch teau, S. Chen, A. Corsi, A. Delbart, J.-M. Gheller, A. Giganon, A. Gillibert, V. Lapoux, T. Motobayashi, M. Niikura, N. Paul, J.-Y. Rouss , H. Sakurai, C. Santamaria, D. Steppenbeck, R. Taniuchi, T. Uesaka, T. Ando, T. Arici, A. Blazhev, F. Browne, A. Bruce, R. J. Carroll, L. X. Chung, M. L. Cort s, M. Dewald, B. Ding, F. Flavigny, S. Franchoo, M. G rska, A. Gottardo, A. Jungclaus, J. Lee, B. D. Linh, J. Liu, Z. Liu, C. Lizarazo, S. Momiyama, K. Moschner, S. Nagamine, N. Nakatsuka, C. Nita, C. R. Nobs, L. Olivier, Z. Patel, Z. Podoly k, M. Rudigier, T. Saito, C. Shand, P.-A. S derstr m, I. Stefan, V. Va-



- quero, K. Wimmer, and Z. Xu, *Phys. Rev. C* **96**, 011301 (2017).
- [57] E. McCutchan, *Nuclear Data Sheets* **125**, 201 (2015).
- [58] J. Tuli and E. Browne, *Nuclear Data Sheets* **157**, 260 (2019).
- [59] A. Korgul, K. P. Rykaczewski, R. Grzywacz, H. Sliwi, J. C. Batchelder, C. Bingham, I. N. Borzov, N. Brewer, S. Liu, C. Mazzocchi, J. A. Winger, and M. Woli, *Physical Review C* **88**, 044330 (2013).
- [60] B. Singh and J. Chen, *Nuclear Data Sheets* **116**, 1 (2014).
- [61] A. Negret and B. Singh, *Nuclear Data Sheets* **124**, 1 (2015).
- [62] W. Urban, K. Sieja, G. S. Simpson, T. Soldner, T. Rząca-Urban, A. Złomaniec, I. Tsekhanovich, J. A. Dare, A. G. Smith, J. L. Durell, J. F. Smith, R. Orlandi, A. Scherillo, I. Ahmad, J. P. Greene, J. Jolie, and A. Linneman, *Physical Review C - Nuclear Physics* **85**, 014329 (2012).
- [63] T. Kibédi, T. Burrows, M. Trzhaskovskaya, P. Davidson, and C. Nestor, *Nuclear Instruments and Methods in Physics Research Section A: Accelerators, Spectrometers, Detectors and Associated Equipment* **589**, 202 (2008).
- [64] S. Hilaire and M. Girod, *European Physical Journal A* **33**, 237 (2007).
- [65] P. Möller, A. J. Sierk, T. Ichikawa, and H. Sagawa, *Atomic Data and Nuclear Data Tables* **109-110**, 1 (2016).
- [66] B. A. Brown and W. D. M. Rae, “In the package, nushell@msu (unpublished),” (2014).
- [67] N. Shimizu, T. Mizusaki, Y. Utsuno, and Y. Tsunoda, *Computer Physics Communications* **244**, 372 (2019).
- [68] B. A. Brown and W. D. M. Rae, *Nuclear Data Sheets* **120**, 115 (2014).
- [69] C. Mazzocchi, A. Korgul, K. P. Rykaczewski, R. Grzywacz, P. Bączyk, C. R. Bingham, N. T. Brewer, C. J. Gross, C. Jost, M. Karny, M. Madurga, A. J. Mendez, K. Miernik, D. Miller, S. Padgett, S. V. Paulauskas, D. W. Stracener, and M. Wolińska-Cichocka, *Acta Physica Polonica B* **46**, 713 (2015).
- [70] M. F. Alshudifat, R. Grzywacz, M. Madurga, C. J. Gross, K. P. Rykaczewski, J. C. Batchelder, C. Bingham, I. N. Borzov, N. T. Brewer, L. Cartegni, A. Fijałkowska, J. H. Hamilton, J. K. Hwang, S. V. Ilyushkin, C. Jost, M. Karny, A. Korgul, W. Królas, S. H. Liu, C. Mazzocchi, A. J. Mendez, K. Miernik, D. Miller, S. W. Padgett, S. V. Paulauskas, A. V. Ramayya, D. W. Stracener, R. Surman, J. A. Winger, M. Wolińska-Cichocka, and E. F. Zganjar, *Physical Review C* **93**, 044325 (2016).
- [71] A. Gilbert and A. G. W. Cameron, *Canadian Journal of Physics* **43**, 1446 (1965).
- [72] T. Kawano, S. Chiba, and H. Koura, *Journal of Nuclear Science and Technology* **43**, 1 (2006).